TECHNICAL REPORT
Project ID #0003018009 VOLUME II

THEORY AND TESTING FOR THE FIRE BEHAVIOR OF MATERIALS FOR THE TRANSPORTATION INDUSTRY

By
A. Tewarson, FM Global, Norwood, MA, USA
J.G. Quintiere, University of Maryland, College Park, MD, USA
D. A. Purser, Fire Safety Engineering Centre BRE, Garston, Watford, UK

Prepared for
Motor Vehicle Fire Research Institute
Attention: Ken Digges, President
1334 Pendleton Court, Charlottesville, VA, USA

October 2005

TECHNICAL REPORT
Project ID #0003018009, VOLUME II

THEORY AND TESTING FOR THE FIRE BEHAVIOR OF MATERIALS FOR THE TRANSPORTATION INDUSTRY

By
A. Tewarson
FM Global, Norwood, MA, USA

J.G.Quintiere
University of Maryland
College Park, MD, USA

D.A. Purser
Fire Safety Engineering Centre BRE
Garston, Watford, UK

Prepared for:
Motor Vehicle Fire Research Institute
Attention: Ken Digges, President
1334 Pendleton Court
Charlottesville, VA, USA

October, 2005

Project ID 0003018009-2

Approved by:

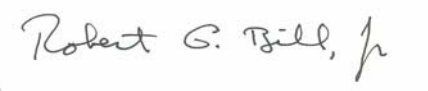

Robert G. Bill, Jr.
Assistant Vice President and Director
Measurements and Models Research

DISCLAIMER

This information is made available for informational purposes only. Reference to specific testing products is not and should not be construed as opinion, evaluation or judgment by FM Global Technologies LLC. FM Global (a) makes no warranty, express or implied, with respect to any products referenced in this report, or with respect to their use, and (b) assumes no liability by or through the use of any information or products referenced in this report.

ABSTRACT

Published results from the reports of the research studies sponsored by General Motor Corporation (GM), National Highway Traffic Safety Administration (NHTSA) and Motor Vehicle Fire Research Institute (MVFRI) have been reviewed to assess the passenger survivability in vehicle crash fires. The results from the review are presented in three reports:

1) Volume I: Post Collision Motor Vehicle Fires;
2) Volume II: Theory and Testing for the Fire Behavior of Materials for the Transportation Industry;
3) Volume III: Thermophysical and Fire Properties of Motor Vehicle Plastic Parts and Engine Compartment Fluids

This volume deals with the theory and testing for the materials used in the transportation Vehicles. There are three chapters in the volume dealing with: 1) theory for the fire behavior of materials; 2) toxicity test methods, and 3) test methods for the fire behavior of materials for the transportation industry.

The theoretical analysis for the fire behavior of materials suggests that the fire hazard potential of materials can be characterized by several measurable parameters, which are related to the ignition, combustion, and flame spread behaviors. These parameters are the heat release parameter (**HRP**), thermal response parameter (**TRP**)**,** critical heat flux (**CHF**), thickness, and ignition length. A combination of the **HRP, TRP**, and heat flux values is related to the flame spread behavior of materials and is expressed as the fire propagation index (**FPI**). Values of **HRP** and **TRP** can be measured in the two advanced ASTM test methods, i.e., ASTM E1354 (the Cone Calorimeter) and ASTM E2058 (FPA).

The review of five test methods for the toxicity testing of vehicle polymers and polymer parts suggest that tests in the ASTM E2058 FPA and ISO/IEC 60695-7-60 provide data directly applicable to the assessment of toxic hazards in vented and unvented fires typical of vehicle fires. Thus, either method could be selected as a standard test method for toxicity.

The National Highway Traffic Safety Administration (NHTSA), Federal Aviation Administration (FAA), Federal Railroad Administration (FRA), Federal Transit Administration (FTA) and US Coast Guard (USCG) specify about 11 different types of tests for small-scale fire testing of materials used in various transport vehicles for flame spread and smoke. Several other tests for flame spread and smoke are used by other testing agencies. The material acceptance

criteria for flame spread and smoke in all these tests are based on low heat exposure conditions, contrary to the conditions in the large scale vehicle fires and thus the testing results do not represent the behaviour of materials typical of these fires.

The ASTM E2058 FPA based 4910 standard of the FM Approvals has been responsible for introducing fire hardened plastic parts in clean rooms of the semiconductor industry world wide. The parts made of 4910 plastics are used in clean rooms without sprinkler protection. The same approach can be taken by the automobile industry, except that acceptance criteria for **FPI** would be higher than for the semi-conductor industry. A **FPI** value $\leq$ 10 $(m/s^{1/2})/(kW/m)^{2/3}$ is recommended as the acceptance criteria of plastics for automobile parts, based on the limited fire spread behavior observed in the large scale tests. The material acceptance criteria could also include limited release of smoke and toxic products based on the smoke and toxic product yields.

All the reports generated in the studies sponsored by GM are listed in the NHTSA web page (www.nhtsa.dot.gov,) and studies sponsored by NHTSA and MVFRI in the MVFRI web page (www.mvfri.org).

ACKNOWLEDGMENTS

Continued encouragements and technical support from Dr. K. H. Digges and Dr. R.R. Stephenson of the Motor Vehicle Fire Research Institute (MVFRI) are gratefully acknowledged. We are also thankful to Mrs. Cheryl McGrath and Mrs. Lisa Ouellet of FM Global for painstakingly assembling various chapters of the report from three authors.

EXECUTIVE SUMMARY

A review has been performed for the results of research studies on the thermophysical and fire properties of vehicle plastic parts and engine compartment fluids, burning behavior of vehicle plastic parts and vehicle burn tests, sponsored by the General Motor Corporation (GM), National Highway Traffic Safety Administration (NHTSA) and Motor Vehicle Fire Research Institute (MVFRI). The studies were undertaken by the GM Research Laboratories, National Institute of Standards, Technology (NIST), FM Global, and the Southwest Research Institute (SwRI). This volume presents the theoretical analysis and testing for the fire behavior of materials for the transportation industry.

Various branches of the Department of Transportation, i.e., the National Highway Traffic Safety Administration (NHTSA), Federal Aviation Administration (FAA), Federal Railroad Administration (FRA), Federal Transit Administration (FTA) and US Coast Guard (USCG) specify about 11 different types of small-scale fire tests for materials used in various transport vehicles, dealing mostly with flame spread and smoke. For the automobile, the FMVSS 302 test is the NHTSA regulatory test for the acceptance of materials in the occupant compartment. Almost all the tests specify limited flame spread under low heat exposure conditions as the material acceptance criterion. Smoke optical density is also specified for the material acceptance criterion in some of the tests.

The flame spread and release of smoke are governed by the heat flux from the flame and other sources and the following parameters that can be measured in the two advanced ASTM test methods, i.e., ASTM E1354 (the Cone Calorimeter) and ASTM E2058 (FPA):

1) Critical heat flux for ignition (**CHF**), which is the minimum heat flux at or below which the material cannot be ignited. If the materials are exposed to heat fluxes that are less than the **CHF** values of the materials or if the materials have high **CHF** values, it is expected that there would be limited or no flame spread beyond the ignition zone in the vehicle crash fires or in the DOT regulatory tests;
2) Heat release parameter (**HRP**), which is the ratio of the heat of combustion to heat of gasification. **HRP** multiplied by the heat flux to which the material is exposed, is equal to the heat release rate. Heat release rate provides the energy ahead of the flame front for flame spread beyond the ignition zone. Materials with low **HRP** values are expected to have limited or no flame spread beyond the ignition zone;

3) Thermal response parameter (**TRP**) for thermally thick behaving materials is the combination of the ignition or decomposition temperature above ambient, density, thermal conductivity, and heat capacity of the material. **TRP** relates to the delay in the ignition of a material for a specified heat flux exposure above the **CHF** value. Materials with high **TRP** values are expected to have limited or no flame spread beyond the ignition zone;
4) A combination of the **HRP**, **TRP**, and the heat flux, to which the material is exposed, is related to the flame spread behavior of the material and is expressed as the fire propagation index (**FPI**) value for the material. An examination of the flame spread behavior in large-scale tests, described in Volumes I and III, indicate that there is limited flame spread beyond the ignition zone for materials with **FPI** values between 6 and 10 $(m/s^{1/2})/(kW/m)^{2/3}$ (for materials with **FPI** values $\leq$ 6 $(m/s^{1/2})/(kW/m)^{2/3}$, there is no flame spread beyond the ignition zone (Chapter III, Section 3-2-6). Based on the vehicle burn test data, limited flame spread is acceptable for the plastic parts. Thus, **FPI** $\leq$ 10 $(m/s^{1/2})/(kW/m)^{2/3}$ is recommended as an acceptance criterion for the plastics for the automobile parts, as discussed in Volume III;
5) Thickness and ignition length, which are related to the thermally thick or thin behaviors and ignition source strength;
6) For the escape of passengers from the vehicle crash fires, visibility through smoke is necessary, which depends on the smoke concentration. For a defined volume, smoke concentration is governed by the yield of smoke and extent of flame spread. For the most common plastics used in the automobile parts, such as polyethylene, polypropylene, and nylon, the yields of smoke $\leq$ 0.06 g/g;
7) The analysis of data from the vehicle burn tests suggest that in vehicle crash fires, untenable conditions created in the passenger compartment are due to heat rather than due to toxic compounds. However, under certain conditions, toxicity may be important. A review of five toxicity test methods suggests that the ASTM E2058 FPA and ISO/IEC 60695-7-60 test standards provide data directly applicable to the assessment of toxic hazards in vehicle fires. Thus, either method could be selected as a standard test method for toxicity;

8) Based on the examination of the pertinent DOT regulatory test methods and conditions that are expected to occur in vehicle crash fires, either the ASTM E ASTM E1354 (the Cone Calorimeter) or the ASTM E2058 (FPA) standard test method is recommended for consideration for inclusion in the possible future DOT regulatory test standards. However, the Cone Calorimeter has limitation in terms of the measurements for the FPI values of the plastics.

This volume has been organized in three chapters as follows:

Chapter I	Theory of Material Fire Behavior;
Chapter II	Toxicity Test Methods;
Chapter III	Test Methods for the Fire Behavior of Materials for the Transportation Industry.

TABLE OF CONTENTS

LIST OF TABLES

LIST OF FIGURES

CHAPTER I
THEORY FOR THE FIRE BEHAVIOR OF MATERIALS

J. G. Quintiere, University of Maryland, College Park, MD, USA

1.1 INTRODUCTION

Material flammability is measured by a variety of test methods, too numerous to consider here. These tests measure a variety of factors from time to ignition, speed of flame spread, how far a flame travels, at what heat flux does it stop, and by various measures that combine several factors. None of these tests provides a complete measure, nor a useful measure for engineering prediction purposes, to be complete or sufficiently general. However, it can be shown that material properties do underlie the processes comprising the flammability of a material. These processes include:

- ignition,
- burning rate per unit area,
- energy release rate (firepower),
- flame spread.

Ignition is characterized by the time to ignite ($\mathbf{t_{ig}}$) and the associated heat flux ($\dot{\mathbf{q}}''$). Burning rate per unit area ($\dot{\mathbf{m}}''$) is a direct result of the heat flux received and the energy required to vaporize the material (**L**). **L** can be defined as

$$\mathbf{L} = \dot{\mathbf{q}}''/\dot{\mathbf{m}}'' \tag{1}$$

where $\dot{\mathbf{q}}''$ is the net heat absorbed to produce the mass flux of the fuel gases, $\dot{\mathbf{m}}''$. The firepower per unit area is then given in terms of a heat of combustion, $\Delta \mathbf{h}_c$, as

$$\dot{\mathbf{Q}}'' = \dot{\mathbf{m}}''\Delta \mathbf{h_c} . \tag{2}$$

These properties, **L** and $\Delta \mathbf{h}_c$, are measurable and true thermodynamic properties for liquid materials but not necessarily exact for solids. However, it has been shown that effective values can be derived from test data to give meaningful values of **L** and $\Delta \mathbf{h_c}$ for solids despite phase change, production of char, and transient effects. Such properties represent average behavior over the flaming period of solids, and have been shown to be generally independent of heat flux during burning even in vitiated atmospheres.

Similarly the processes of ignition and flame spread can be represented in terms of thermal properties needed to heat the material to its ignition temperature namely, these thermal properties include

- density, ρ;
- specific heat, **c**;
- conductivity, **k**.

As we shall see the thickness of the material, δ, and its heat transfer characteristics will also be important. The concept of an ignition temperature comes directly from the gas phase test results for auto-ignition temperature of a solid, which is associated with the ability to ignite, and as in the flash point, where vaporized fuel at its lower flammability limit is ignited by a pilot flame. For a higher temperature, with the correct fuel vapor concentration, a minimum temperature for auto-ignition can be associated with the gas mixture and related to the surface temperature. Hence, an auto-ignition surface temperature can be ascertained. To the extent that these critical temperatures for a solid fuels' surface at pilot or auto-ignition do not vary over a range of heating conditions, then these temperatures might be considered material properties. Indeed, the test procedure offered by ASTM E 1321 [1] (LIFT) gives a means to measure $\mathbf{k\rho c}$, and $\mathbf{T_{ig}}$ under ignition and opposed flow spread. The ASTM E 2058 [2] has been used to measure **L** and $\mathbf{\Delta h_c}$ for materials, as well as other properties related to the production of combustion products as "yields". The yields give the stoichiometry of the fire reaction based on the mass lost to vapor, i.e.

$$\mathbf{y_i = \frac{m_i}{m_{lost}}} \tag{3}$$

These yields are distinct from true stoichiometric coefficients that are in terms of mass reacted. It should be noted that the properties **L** and $\mathbf{\Delta h_c}$ are also based on the mass loss of fuel to vapor. All of the vapor may not be fuel as some fuel might contain noncombustible components, such as water vapor released on decomposition from say ammonium tri-hydrate – a retardant. In the ASTM E 2058, as in the ASTM E 1354 [3], the chemical energy release rate is measured based on the consumption of oxygen ($\mathbf{\dot{m}_{ox}}$) and using $\mathbf{\Delta h_{ox}} \approx 13.1$ kJ/g oxygen reacted. Then

$$\mathbf{\Delta h_c \equiv \frac{\dot{Q}_{chem}}{\dot{m}_{lost}} = \frac{\dot{m}_{ox}\Delta h_{ox}}{\dot{m}_{lost}}}, \tag{4}$$

and **L** is given as before by the linearity between mass loss rate and applied heat flux.

The ability to measure properties associated with fire conditions of solid (or liquid) materials allows the generalization of fire test results to applications in problem solving and hazard assessment. The material properties pertaining to flammability might be represented as

- heat of combustion, Δh_c
- heat of gasification, **L**
- thermal inertia, $k\rho c$
- Vaporization temperature, T_v
- ignition (pilot) temperature, T_{ig}.

Table 1-1 gives typical values for these properties.

Table 1-1. Typical Material Fire Properties

Property (units)		Liquids	Melting Solids	Charring Solids
Δh_c	(kJ/g)	20 – 40	20 – 40	5 – 15
L	(kJ/g)	0.5 – 1	1 – 3	5 – 8
T_v	(°C)	100 – 400	250 – 400	350 – 500
T_{ig} (pilot)	(°C)	(-20) – 200	200 – 350	250 – 400
T_{ig} (auto)	(°C)	300 – 500	350 – 600	400 – 600

In the early stage of fire growth before the oxygen is likely to be depleted, heat flux from the flame and the surroundings is important for fire growth. Thus, many tests impose a radiant external heat flux $\dot{q}''_e$ to ascertain the behavior of a material related to the early fire growth stage; indeed, many materials will not burn in air without the addition of radiant heat flux. Therefore, to assess the flammability of a material, its behavior under external heating should be fully described.

Many test methods, although incorporating an external heat flux, do not fully represent the materials behavior over a range of heat flux, nor do they represent all of the fire processes for the material. Since it will be shown that the basic fire processes -- ignition, spread, burning -- are all independent, it is essential that they all be measured and described over the appropriate heat flux range for a material. The upper level of heat flux might be representative of flame heat fluxes as high as 50 to 75 kW/m^2 associated with conditions after flashover and at the start of a fully involved room fire. It should be noted that heat fluxes in a test of a material will not

necessarily be the same as those under actual fire conditions. This is where engineering modeling is needed, and the imposition of standard test results for correlating real fire behavior usually ends in an unsatisfactory result. Figure 1-1 illustrates the difference between test and fire heat fluxes. Both the flame and environmental heat fluxes differ between a test and a realistic fire.

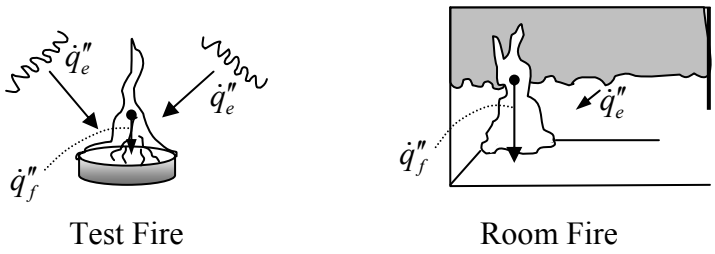

Figure 1-1. Heat fluxes in fire tests and reality.

Recently, work by Panagiotou and Quintiere [4] have shown that the Cone Calorimeter, and a radiant heater apparatus to examine upward and downward flame spread could be used to develop "Flammability Diagrams" of materials to show their full characteristics over a range of heat flux. The lowest heat flux used for each process -- ignition, spread, and burning -- is important to judge the complete flammability behavior of a material. Indeed, the test for floor coverings ASTM E 648 [5] and the new FAA test for aircraft insulation coverings are based on a critical heat flux for spread. Figures 1-2 to 1-5 give examples of Flammability Diagrams [4].

This chapter will illustrate the theory of burning under radiant heating conditions. It will attempt to derive relationships for the various burning processes and their limiting conditions. It will be interesting to see how the material fire properties enter into the results.

1.2 RADIANT HEATING

Radiant heating by the fire, smoke, and heated surfaces is the driving force for fire growth on materials. In fact, many materials will not burn unless they are exposed to a sufficient radiant heat flux. This is why test methods used to examine the performance of materials in fire or exposure to large flame sources incorporate radiant heating of the material. This type of test is in contrast to those using small flame or Bunsen burner sources to only assess ignition and self-propagation under normal ambient conditions. The small flame test only exposes a small sample

area to a significant heat flux. Consequently, issues of burn-out, melting away, or shrinking before ignition can occur, will give no indication of ignition under a large heat exposure. Radiant heating by other test methods provide both a surrogate for large flame heating exposure, and a simulation of the radiant heating in realistic fire conditions. The tests incorporating radiant heating can provide a measure of the material's performance under a range of fire conditions. Since all combustible materials will burn, it is much better to understand how they burn under a spectrum of representative fire heating conditions then simply whether they burn under normal ambient conditions.

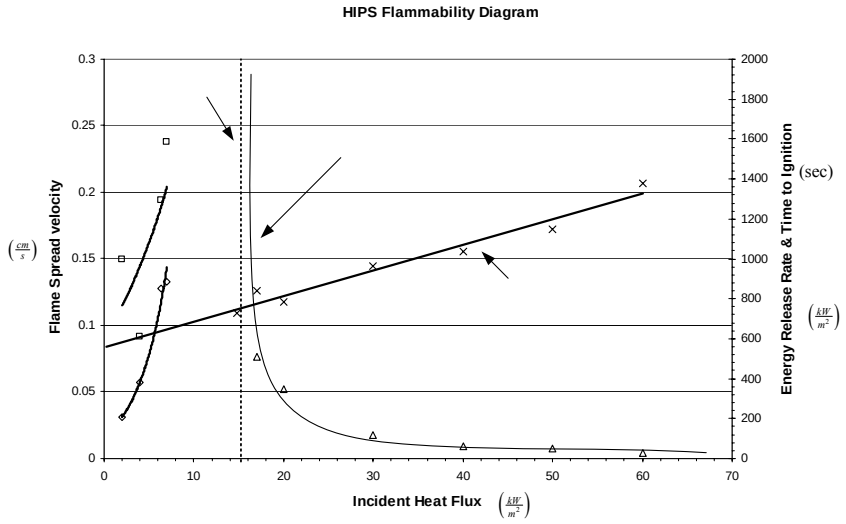

Figure 1-2. High Impact Polystyrene (HIPS) Flammability Diagram [4].

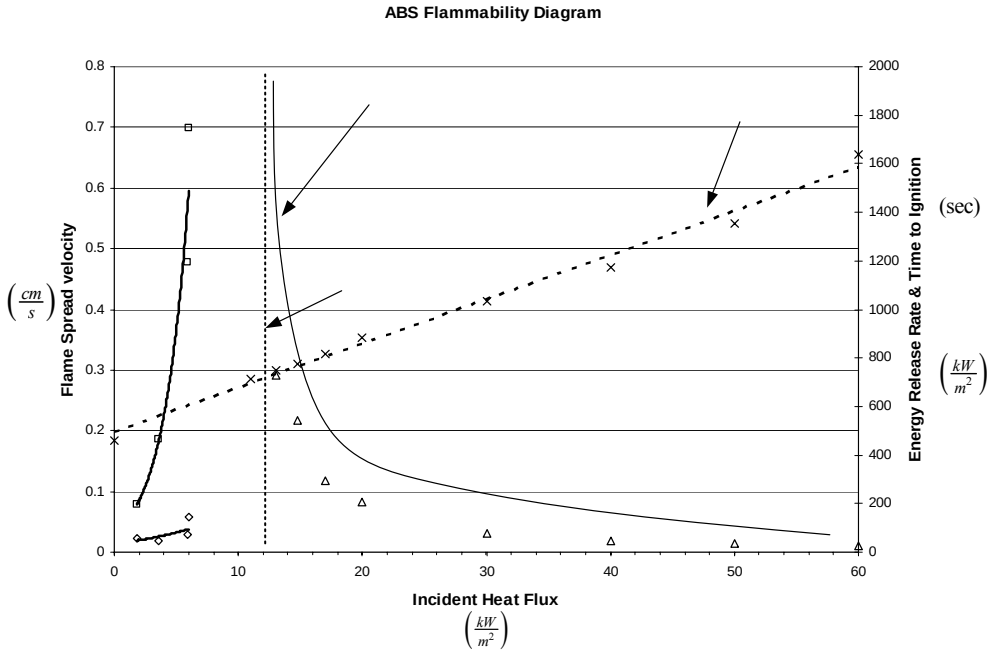

Figure 1-3. Acrylonitrile Butadiene Styrene (ABS) Flammability Diagram [4].

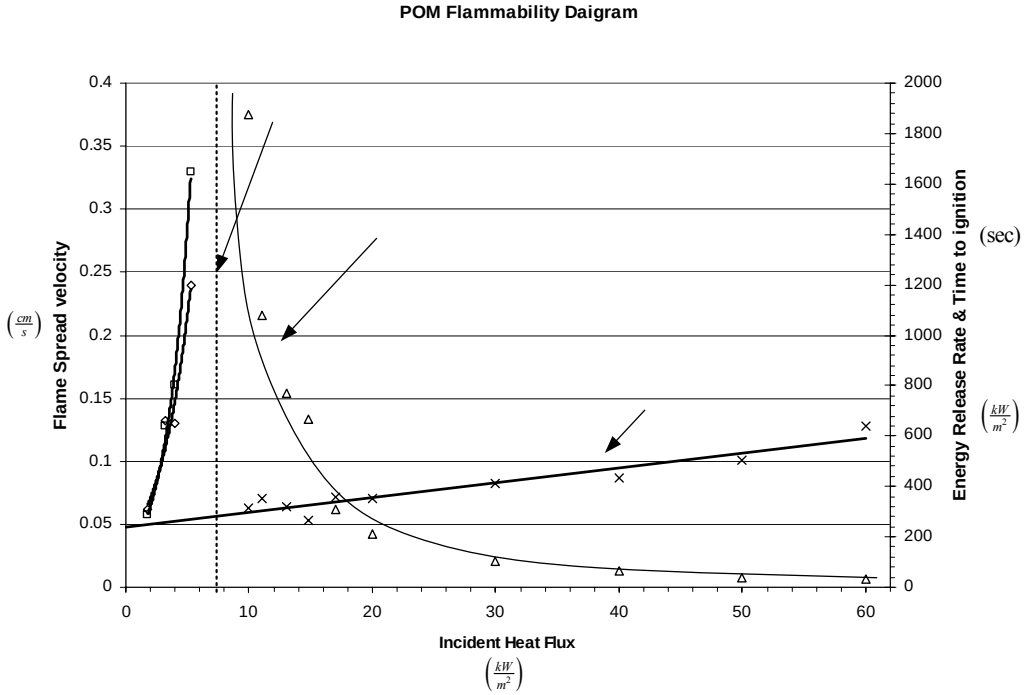

Figure 1-4. Polyoxymethylene (POM) Flammability Diagram [4].

UP

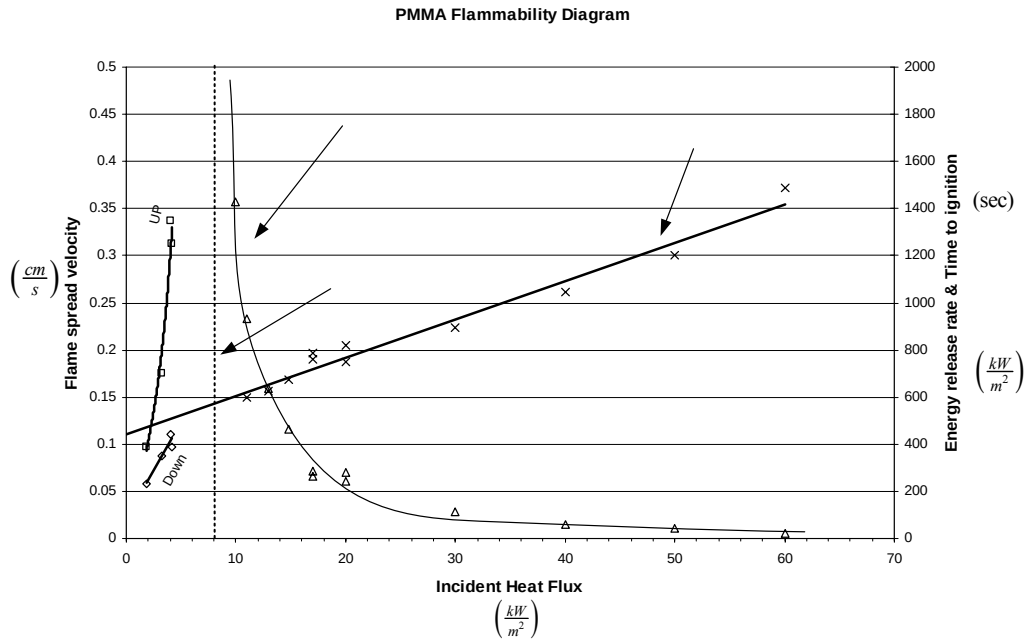

Figure 1-5. Polymethylmethacrylate (PMMA) Flammability Diagram [4].

1.2.1 Heating Model

Let us consider the theory of heating a condensed phase - solid or liquid material -- by a constant incident heat flux, $\dot{\mathbf{q}}''$. This incident heat flux can represent the flame, composed of both convective and radiant flux components, or simply an external heat flux representative of the heating from a radiant test source or from fire conditions. A linear heat loss will be considered based on a constant heat transfer coefficient, $\mathbf{h_t}$. Figure 1-6 shows the heating configuration for a material of thickness, $\boldsymbol{\delta}$, insulated on the back-face.

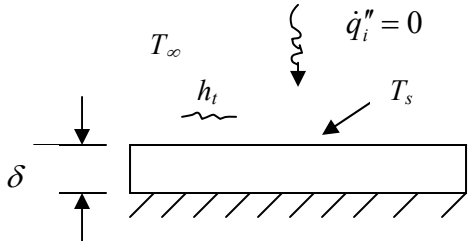

Figure 1-6. Heating of a material.

This heat transfer coefficient can be composed of a convective and radiative component.

For pure radiative heating: $\dot{\mathbf{q}}'' = \dot{\mathbf{q}}_{\mathbf{e}}''$, $\mathbf{h_t} = \mathbf{h_c} + \mathbf{h_r}$.

For flame heating: $\dot{q}'' = \dot{q}''_f = \dot{q}''_{f,c} + \dot{q}''_{f,r}$, $h_t = h_r$ where $h_t = \frac{\sigma(T^4 - T_\infty^4)}{T - T_\infty}$.

1.2.2 Thermally Thin and Thick

Both thermally thin and thermally thick materials will be considered which represent the range of possible physical thicknesses. A thermally thin material ideally has a uniform temperature. It corresponds to physically thin materials, those heated for a long time, or those at the end of a burning process where the virgin material has become thin. A thermally thick material always has a temperature distribution that is not influenced by back-face effects. It corresponds to an infinitely thick domain, the earlier phase of heating, or effectively the heating of a thin combustible material over a thick non-combustible substrate.

1.2.3 Thermally Thin Heating Model

Consider a thermally thin material of thickness, δ, at an initial temperature, T_o, and exposed to an ambient temperature, T_∞. See Figure 1-6. The governing equation is

$$\rho c \delta \frac{dT}{dt} = \dot{q}'' - h_t (T - T_\infty) \tag{5}$$

For the initial condition

$$t = 0,\ T = T_o \tag{6}$$

the solution can be shown as

$$T - T_o = \left[\frac{\dot{q}''}{h_t} - (T_o - T_\infty)\right]\left(1 - e^{-\tau}\right) \tag{6a}$$

where

$$\tau = h_t t / \rho c \delta. \tag{6b}$$

For small τ values,

$$T - T_o = \left[\frac{\dot{q}''}{h_t} - (T_o - T_\infty)\right]\tau. \tag{7}$$

For large τ:

$$T - T_o \approx \frac{\dot{q}''}{h_t} - (T_o - T_\infty) \tag{8a}$$

or $$T - T_\infty \approx \frac{\dot{q}''}{h_t}. \tag{8b}$$

This says for long-time heating at a given heat flux, the temperature will reach an equilibrium temperature above ambient. That equilibrium temperature does not depend on its initial value.

1.2.4 Thermally Thick Heating Model

For the same heating and initial conditions the thick problem is described by

$$\frac{\partial T}{\partial t} = \frac{k}{\rho c}\frac{\partial^2 T}{\partial x^2} \tag{9}$$

$$x = 0,\ -k\frac{\partial T}{\partial x} = \dot{q}'' - h_t\,(T - T_\infty),\ t = 0,\ T = T_o,\ x\to\infty,\ T = T_o$$

Let $\theta = T - T_o$

$$\frac{\partial \theta}{\partial t} = \frac{k}{\rho c}\frac{\partial^2 \theta}{\partial x^2}$$

$$x = 0,\ -k\frac{\partial \theta}{\partial x} = [\dot{q}'' - h_t\,(T_o - T_\infty) - h_t\,\theta\,,]$$

and

$$t = 0,\ x\to\infty,\ \theta = 0.$$

It can be shown that the surface temperature is

$$T_s - T_o = \left[\frac{\dot{q}''}{h_t} - (T_o - T_\infty)\right]\left[1 - \exp(\gamma^2)\,\mathrm{erfc}(\gamma)\right]. \tag{10}$$

where

$$\gamma = h_t\sqrt{\frac{t}{k\rho c}}\,. \tag{11}$$

For large γ – long-time solution,

$$T_s - T_o \approx \left[\frac{\dot{q}''}{h_t} - (T_o - T_\infty)\right]\left[1 - 1/(\sqrt{\pi}\,\gamma)\right]. \tag{12}$$

For small γ – short-time solution,

$$T_s - T_o \approx \left[\frac{\dot{q}''}{h_t} - (T_o - T_\infty)\right]\left(\frac{2}{\sqrt{\pi}}\,\gamma\right). \tag{13}$$

1.2.4.1 Finite Thickness

At some time, an insulated solid of thickness δ will begin to act as a *thermally thin* solid. Previously it acted as a *thermally thick* (semi-infinite) solid. This will occur if it is very thin or

when a thick solid becomes more uniform in temperature later in time. Under the same heating and initial conditions, we can equate the thin and thick solutions to find this time, t_δ. This is done by equating the small-time solutions when the thin temperature is the same as the thick surface temperature.

$$\frac{h_t t}{\rho c \delta} = \frac{2}{\sqrt{\pi}} \frac{h_t \sqrt{t}}{\sqrt{k \rho c}} \tag{14}$$

Thus the time to become thin is

$$t_\delta = (4/\pi)(\delta^2/\alpha),\ \alpha = (k/\rho c) \tag{15}$$

This can be considered the time it takes thermal diffusion to reach the thickness dimension, **δ.**

1.3 IGNITION

The Ignition of solids or liquids can be modeled in terms of an ignition temperature. This can apply to both piloted and auto-ignition. For a liquid, surface temperature that produces the lower flammable limit (LFL) at its surface due to evaporation is called the flash point. A pilot of sufficient heat strength will enable pre-mixed flame propagation at the surface that is usually sufficient to sustain a diffusion flame on the liquid. Under this condition, the flash point can be considered as piloted ignition temperature. The same processes apply to a decomposing solid, but its decomposition chemistry will cause its surface temperature to vary somewhat at the LFL. However, the concept of a *constant* ignition temperature is a good first approximation. Arguments for a constant surface temperature corresponding to auto-ignition can also be made. The auto-ignition is controlled by the temperature and concentration of fuel in the vaporized mixture with air. This gas-phase auto-ignition depends on the temperature of the vaporized fuel leaving its hot surface. Hence, the surface temperature corresponds to the auto-ignition temperature of vapor mixture.

1.3.1 Ignition Model

Ignition under a constant heat flux can then be described by the heating of the condensed-phase to a critical temperature corresponding to piloted or auto-ignition, $\mathbf{T_{ig}}$. It has been found that both the short and long time solutions can be significant in describing ignition. From the heating models, Eqns. (8) and (13), it follows that the surface temperature can be approximately described as

$$T_s - T_o = [\frac{\dot{q}''}{h_t} - (T_o - T_\infty)]F(t). \quad (16)$$

And from the limiting time solutions,

$$F(t) = \tau^n, \quad \tau < \tau^* \qquad \begin{cases} 1, & \tau \geq \tau^* \end{cases} \quad (17)$$

For the thin case, $n = 1$ and $\tau = h_t\, t / \rho c \delta$, and for the thick case, $n = ½$ and $\tau = 4 h_t^2\, t / k\rho c$. At ignition $T_s - T_{ig}$ and the time for ignition (t_{ig}) can be determined. In addition, for long heating at a given heat flux the surface temperature may never achieve its ignition value, This limiting flux to just cause ignition is called the critical flux for ignition, $\dot{q}''_{o,ig}$. From the heating solutions, Eqns. (5b) and (8),

$$\dot{q}''_{o,ig} = h_t\,(T_{ig} - T_\infty) \equiv CHF. \quad (18)$$

Hence, this critical flux depends on the convective heat transfer conditions, and is usually reported for natural convection conditions. Tewarson refers to this parameter as CHF, the critical heat flux for piloted conditions in normal air. For the case of $T_\infty = T_o$, the time to ignition is given by

$$\text{Thin:} \quad t_{ig} = \frac{\rho c \delta (T_{ig} - T_o)}{\dot{q}''}, \; t_{ig} < t^* \quad (19a)$$

$$\text{Thick:} \quad t_{ig} = \frac{\frac{\pi}{4} k\rho c (T_{ig} - T_o)^2}{\dot{q}''}, \; t_{ig} < t^* \quad (19b)$$

Note, in general for pre-heating the surface to T_o, then in the above equation replace $\dot{q}''$ by $\dot{q}'' - h_t (T_o - T_\infty)$. Approximately, $t^* = t_{ig}$ when $\dot{q}''$ is the critical flux. In the thick case, it is seen that the ignition time is related to the Thermal Response Parameter (**TRP**) of Tewarson as

$$t_{ig} = \left(\frac{TRP}{\dot{q}''}\right)^2 \quad (20)$$

1.3.2 Ignition of Vehicle Engine Materials

Three vehicle materials were examined to see how they might follow this theoretical ignition behavior. They are listed in Table 1-2.

Table 1-2. Selected Vehicle Materials

Vehicle Component	Vehicle: Make/Model/Year
Hood liner face (PET)	Dodge/Caravan/1996
Front wheel well liner (PP, PE)	Chevrolet/Camaro/1997
Windshield laminate	Chevrolet/Camaro/1997

Measurements are taken from the results of two standard tests: ASTM E 1354 Cone Calorimeter [3] and ASTM E 1623 ICAL [6]. The latter uses a large vertical sample as compared to the small horizontal sample of the Cone. The convective heat loss coefficients are similar in natural convection for vertical and horizontal samples, so we should not expect differences for ignition from these two tests. Figures 1-7 to 1-9 confirm this expected agreement. It should be noted that the flame configurations are different between the two tests, and results that depend on *flame* heat flux will be different.

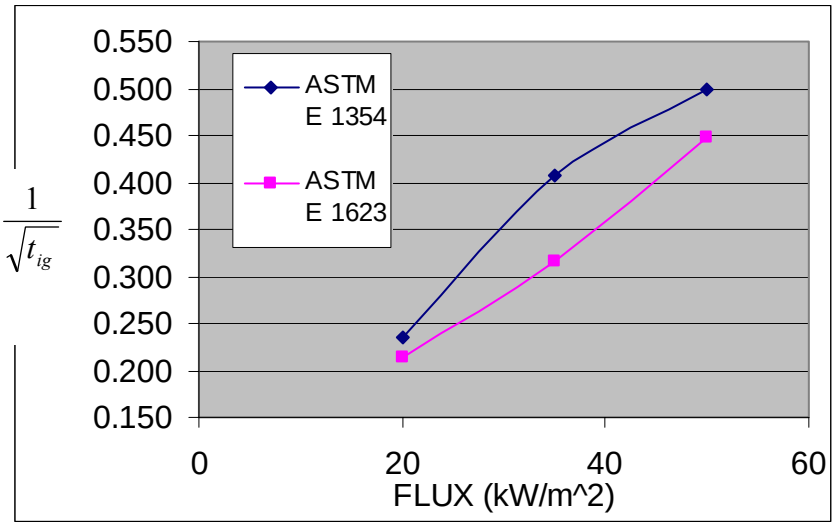

Figure 1-7 Hood liner ignition.

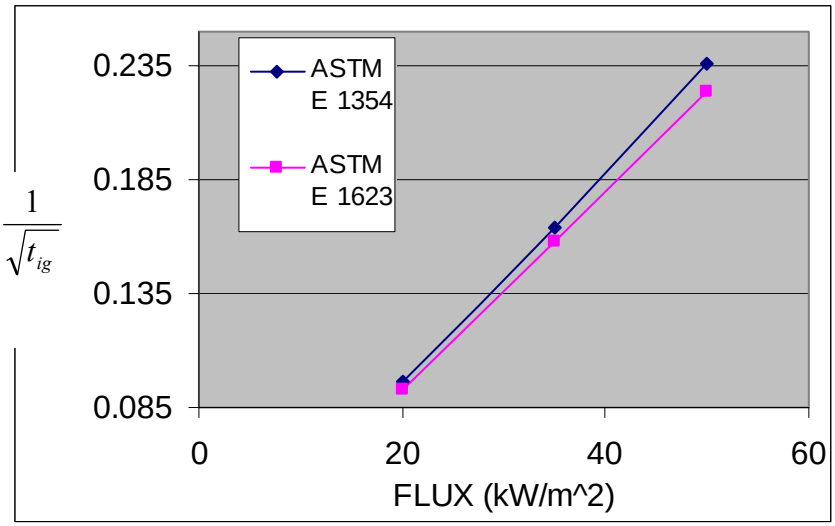

Figure 1-8 Wheel well liner ignition.

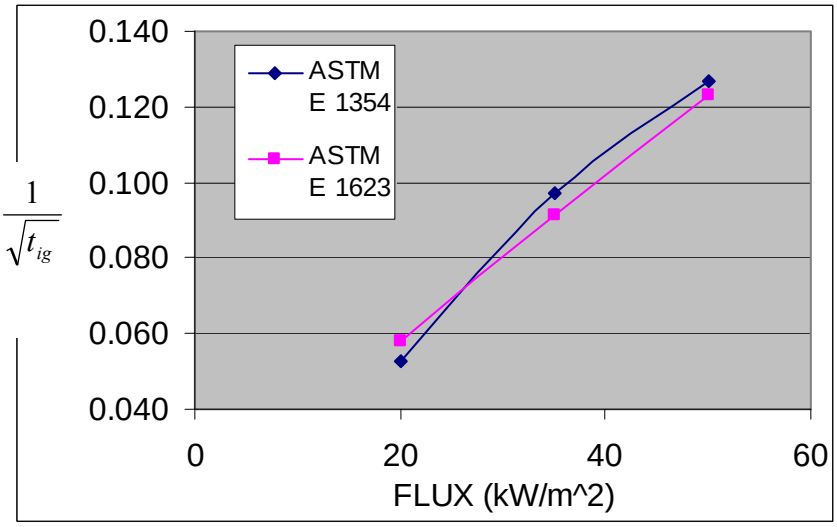

Figure 1-9 Windshield laminate ignition.

1.3.3 Ignition Temperature and Minimum Mass Flux at Piloted Ignition

At piloted ignition the fuel mass fraction near the surface must be at the lower flammable limit of the vaporized fuel. The vaporized mass flow rate per unit area (mass flux), with the mass transfer coefficient given from the convective heat transfer coefficient, is given by

$$\dot{m}''_F = \frac{h_c}{c_p}\left(Y_{F,L} - 0\right) \tag{21}$$

Figure 1-10 illustrates the process.

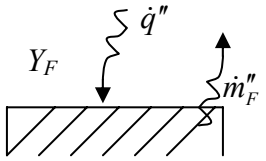

Figure 1-10 Piloted ignition at the LFL.

The lower flammable limit (LFL), $\mathbf{Y_{F,L}}$, can be determined from an empirical correspondence to a critical adiabatic flame temperature of the mixture (usually taken at 1300 °C). The fuel concentration corresponding to the adiabatic flame temperature is

$$\mathbf{Y_{F,L}} = \frac{\mathbf{c_p(T_{f,crit} - T_o)}}{\mathbf{\Delta h_c}}. \tag{22}$$

Hence, the critical mass flux at ignition is

$$\mathbf{\dot{m}''_{o,ig}} = \frac{\mathbf{h_c(T_{f,crit} - T_o)}}{\mathbf{\Delta h_c}} \tag{23}$$

For conditions of natural convection in air the critical mass flux is inversely related to the heat of combustion.

This mass flux must occur at the ignition temperature. For liquids, this temperature is the flashpoint. From the Clausius-Clapeyron equation, the fuel mass fraction at the flashpoint is given by

$$\mathbf{Y_{F,L}} = \mathbf{A_b e}^{-\frac{\mathbf{M_F h_{fg}}}{\mathbf{RT_{ig}}}} \tag{24}$$

where $\mathbf{R}$ is the universal gas constant, $\mathbf{M_F}$ is the molecular weight of the fuel and $\mathbf{h_{fg}}$ is the heat of vaporization and

$$\mathbf{A_b} = \left(\frac{\mathbf{M_g}}{\mathbf{M}}\right)\mathbf{e}^{\frac{\mathbf{M_g h_{fg}}}{\mathbf{RT_b}}} \tag{25}$$

with $\mathbf{M}$, the molecular weight of the mixture and $\mathbf{T_b}$ is the boiling point. Thus, the flashpoint (ignition temperature) can be determined from the relationship

$$\frac{\mathbf{c_p(T_{f,crit} - T_o)}}{\mathbf{\Delta h_c}} = \mathbf{A_b e}^{-\frac{\mathbf{M_F h_{fg}}}{\mathbf{RT_{ig}}}}. \tag{26}$$

A similar result for a thermally decomposing solid with its kinetics described by an Arrhenius reaction as the fuel decomposition rate per unit volume is

$$\dot{m}_F''' = Ae^{-\frac{E}{RT}} \quad . \tag{27}$$

The surface mass flux is related to the decomposition rate per unit volume by

$$\dot{m}_F'' = \int_0^\infty \dot{m}_F''' dx \, . \tag{28}$$

Treating this vaporized fuel concentration at the LFL as was done for the liquid gives

$$\frac{c_p(T_{f,crit} - T_o)}{\Delta h_c} = \left(\frac{c_p A}{h_c}\right) \int_0^\infty e^{-\frac{E}{RT}} dx \, . \tag{29}$$

It can be seen that the temperature of the surface at ignition depends upon the temperature distribution or the rate of heating. Hence, the piloted ignition is not exactly a constant for a decomposing solid. If the heating rate is high enough to cause a thin decomposition zone, then a constant ignition temperature is more likely.

1.4 BURNING RATE PER UNIT AREA, $\dot{m}_F''$

As in the modeling of ignition, liquid burning behavior is used to describe the general burning of materials as an ideal representation. This ignores transient effects, primarily due to charring, and phase change is always considered from the original solid to fuel vapor in one step. This model of burning represents the time-average or peak burning conditions in a reasonable sound engineering format. An analysis of steady burning with external radiant heating for this idealized liquid model can be expressed as follows:

$$\dot{m}_F'' L = \dot{q}_{f,c}'' + \dot{q}_{f,r}'' + \dot{q}_e'' - \sigma(T_v^4 - T_\infty^4) \, . \tag{30}$$

This pertains to the sketch in Figure 1-11. Flame heating by convection and radiation is distinguished.

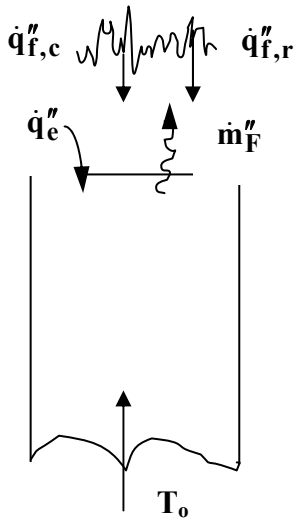

Figure 1-11 Steady Burning.

1.4.1 Heat of Gasification

The energy needed to vaporize must be balanced by the net heating to the surface. The heat of gasification (**L**) for a liquid is composed of two terms in steady burning: (1) the heat of vaporization, ($\mathbf{h_{fg}}$) at the boiling point ($\mathbf{T_b}$) and (2) the energy needed to raise the original material to its boiling point from its initial temperature. For a liquid,

$$\mathbf{L = h_{fg} + c(T_b - T_o),} \tag{31a}$$

and in general,

$$\mathbf{L = \Delta h_v + c(T_v - T_o)} \tag{32}$$

where $\mathbf{\Delta h_v}$ is an overall enthalpy change needed to vaporize the solid, and $\mathbf{T_v}$ is the decomposition temperature.

As in ignition, the decomposition or surface temperature at vaporization during steady burning is not a precise constant, but can vary over a range. For charring materials, **L** is truly an effective property that includes both transient char build up and decomposition. Nevertheless, bulk properties can be measured as Tewarson uses the Heat Release Parameter (**HRP**) $\equiv \mathbf{\Delta h_c / L}$ for materials. The measured properties are found for time-averaged results, and they are consistent with the theoretical model here, as well as models that are likely to be used in engineering analyses.

1.4.2 Flame Convection

It can be shown for a one-dimensional diffusion flame (stagnant layer model) that the flame heat flux can be represented as [7]

$$\dot{q}''_{f,c} = h_c\left[\left(\frac{(1-X_r)Y_{ox,\infty}\Delta h_c}{rc_p}\right)-(T_v-T_\infty)\right]\approx h_c(T_f-T_v). \tag{33}$$

Here $Y_{ox,\infty}$ is the ambient oxygen mass fraction, and h_c is the convective heat transfer coefficient of the flame. The convective flame heat flux incorporates a flame radiation fraction defined as

$$X_r = \frac{\dot{Q}_r}{\dot{m}_F\Delta h_c} \tag{34a}$$

where $\dot{Q}_r$ is the rate of flame energy radiated away. This can be considered a fuel property, although it can depend on scale. The stoichiometric oxygen to fuel mass ratio, **r**, can be given as

$$r = \frac{\Delta h_c}{\Delta h_{ox}} \tag{34b}$$

where $\Delta h_{ox} \approx 13.1$ kJ/g oxygen reacted. However, in Eq. (34b), **r** can be effectively higher than its chemical value due to turbulent mixing of fuel and oxygen. From convective heating, the flame temperature may be estimated by

$$c_p(T_f-T_\infty)\approx\frac{Y_{ox,\infty}(1-X_r)\Delta h_c}{r}. \tag{35}$$

1.4.3 Flame Radiation

Flame radiation can be represented as a homogenous, gray gas flame with a mean beam length, L_e. Let us consider a fire plume as a cylindrical flame, and a boundary layer flame as a thin layer. See Figures 1-12a and 1-12b.

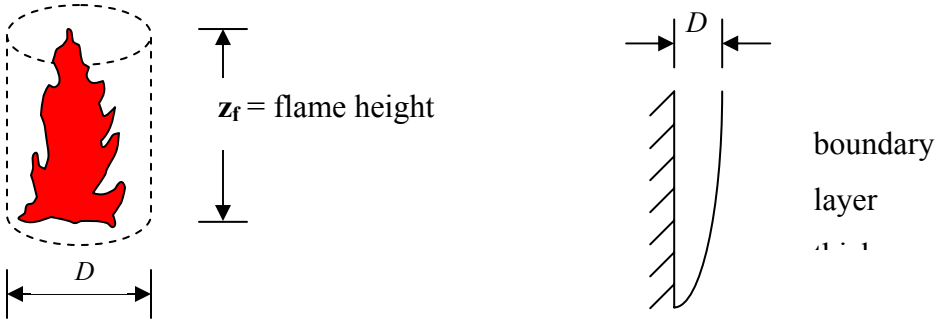

Figure 1-12 a and b Flames in radiation modeling

In general we can represent the flame radiative heat flux as

$$\dot{q}''_{f,r} = (1 - e^{-\kappa L_e})\sigma(T_f^4 - T_\infty^4) \tag{36}$$

where T_∞ is the ambient temperature, T_f is the flame temperature, and κ is the flame absorption coefficient (m^{-1}). From Siegel and Howell [8] it can be determined that for an infinite slab, or the approximate boundary layer flame,

$$L_e = 1.8\ D \qquad (D = \delta_{BL}), \tag{37a}$$

and for a cylindrical flame of diameter, D and height, z_f , an approximate fit to view factor results gives

$$L_e = D[0.65(1 - e^{-2.2\left(z_f / D\right)})] \tag{37b}$$

1.4.4 Interpretation of Test Data for Burning Rate

In the Cone Calorimeter, for a horizontal sample with $z_f > D$, in most cases $L_e \approx 0.65\ D$. Thus, both the small vertical and horizontal samples burning in the Cone Calorimeter will have $\dot{q}''_{f,r} \approx$ constant for a given D, material size, since the beam length and flame emissivity are then constants. Also $\dot{q}''_{f,c}$ will be approximately constant for a given sample, since h_c depends only on geometry and flow. Therefore, a data plot of peak-average (or quasi-steady) burning flux can give L and $\dot{q}''_{f,net}$ in the Cone Calorimeter or in similar fire test methods. This is shown below in Figure 1-13, and follows from Eq. (30).

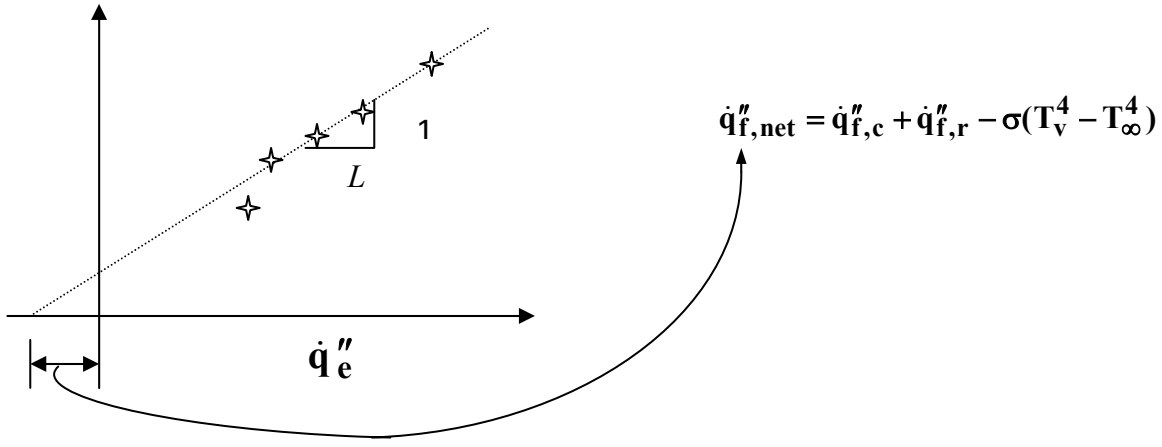

Figure 1-13 Typical peak mass loss rate data.

As the Cone Calorimeter determines the chemical energy flux (or heat release rate HRR), $\dot{\mathbf{Q}}''$, the heat of combustion is readily determined by

$$\Delta \mathbf{h_c} = \frac{\dot{\mathbf{Q}}''}{\dot{\mathbf{m}}_{\mathbf{F}}''} . \tag{38}$$

Even for unsteady, charring materials, we can derive effective properties that can be used to predict or reproduce the peak burning conditions. In summary, we can obtain from the Cone Calorimeter: $\Delta \mathbf{h_c}$, $\mathbf{L}$, and $\dot{\mathbf{q}}''_{\mathbf{f,net}}$.

Figure 1-14 shows the peak mass loss flux for the vehicle materials given in Table 1-3. Theory suggests, for a measurable **L**, the behavior would be linear with the heat flux. The headliner material departs from this trend at a flux of 50 kW/m^2. This behavior suggests more a problem with these data, than with the theory, as these trends have been demonstrated for materials in general.

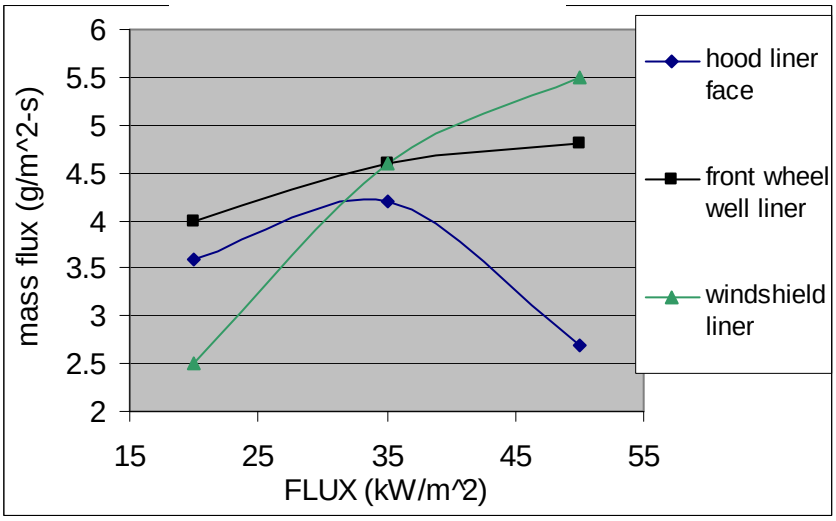

Figure 1-14 Mass flux for vehicle materials from the Cone Calorimeter.

The energy flux is given by Eq. (38) and alternatively in oxygen calorimetry as

$$\dot{\mathbf{Q}}'' = \frac{\dot{\mathbf{m}}_{\mathbf{ox}} \Delta \mathbf{h}_{\mathbf{ox}}}{\mathbf{A_F}} \tag{39}$$

where $\dot{m}_{ox}$ is the oxygen depletion rate, and A_F is the fuel area vaporizing. Consequently, peak energy flux should follow a similar behavior to mass flux and heat flux from Eqs. (30) and (38)

$$\dot{Q}'' = \dot{q}''_{net}\left(\frac{\Delta h_c}{L}\right), \tag{40}$$

where $\frac{\Delta h_c}{L}$ is the Heat Release Parameter of Tewarson, **HRP**. This parameter can be obtained from the slope of energy and heat flux data. Such data are shown for the vehicle materials in Figures 1-15 to 1-17.

All the data are monotonic increasing with heat flux, unlike the anomaly for the mass flux of the hood liner. Here, results from the ICAL are shown with the Cone Calorimeter. For **HRP** to be a true property, the data from each apparatus should be parallel for a given material. This is only apparent for the windshield laminate. As the validity of a constant **HRP** has been generally established, the data need to be questioned here. Also, the flame heat fluxes will be different due to the size and configuration differences of the samples in each test method. It might be expected that one flame would consistently have a higher heat flux than that in the other device. This consistency is not displayed in these results, as only two are consistent.

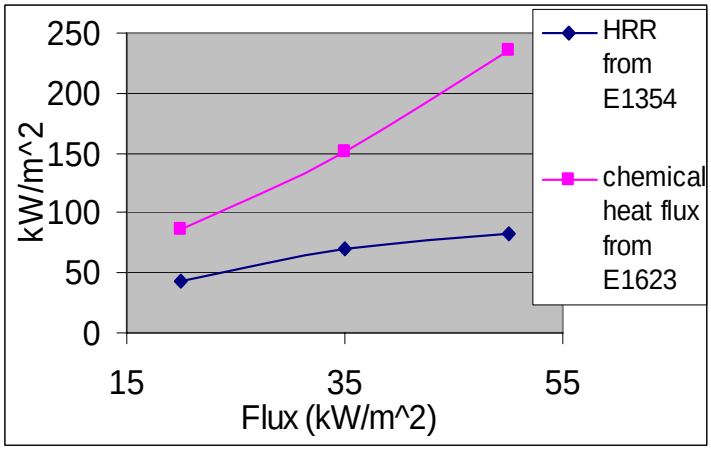

Figure 1-15 Energy flux for hood-liner

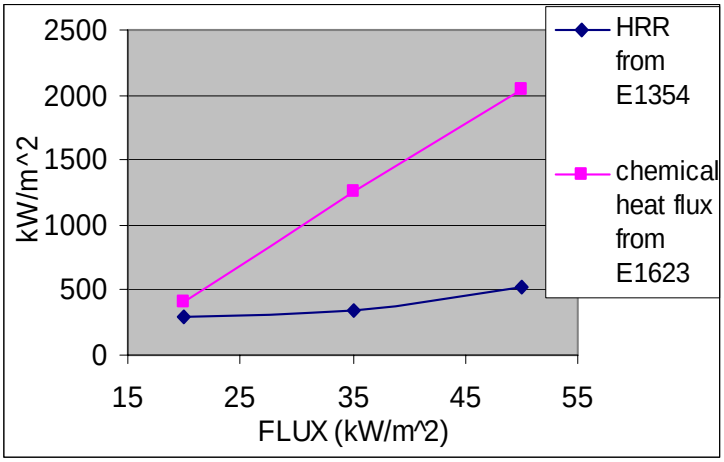

Figure 1-16 Energy flux from wheel-liner

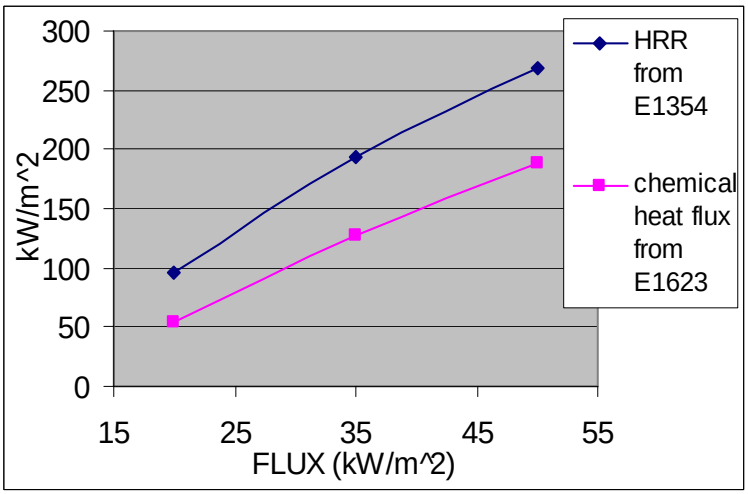

Figure 1-17 Energy flux from windshield laminate

It should be mentioned here that all these materials pass the small flame ignition test in DOT FMVSS 302 [9], but only the wheel well liner has a non-zero burning rate (37 mm/min). From the Cone data, **HRP** was computed and compared to the FMVSS 302 test results in Table 1-3.

Table 1-3. DOT 302 and HRP Results

Material	**Burning Rate**	**Pass/Fail**	**Cone HRP**
	mm/min		(-)
Hood Liner	0	Pass	7.7
Wheel Liner	37	Pass	53.0
Windshield Laminate	0	Pass	4.3

1.4.5 Critical Mass Flux at Extinction

Consider a material burning under a constant external radiant heat flux. As the external radiant heat flux is reduced (ideally under steady burning), the fuel vaporization rate will decrease, the flame will become smaller and therefore laminar with negligible radiation loss. For pure fuel being vaporized from the condensed-phase, the flame temperature under these conditions is given as [7]

$$c_p(T_{f,crit} - T_\infty) = \frac{Y_{F,o}(1 - X_r)\Delta h_c - L_m + c_p(T_v - T_\infty)}{1 + \frac{r Y_{F,o}}{Y_{ox,\infty}}} \tag{41}$$

where

$$L_m \equiv L - \frac{\dot{q}''_e - \sigma(T_v^4 - T_\infty^4)}{\dot{m}''_F} \tag{42}$$

is a modified heat of gasification to account for the external and re-radiative heat transfer. We assume the fuel gases are pure so $Y_{F,o}$ = 1. (Inert materials in the solid would reduce $Y_{F,o}$). Letting $\dot{q}''_{f,r}$, and $X_r \to 0$ and substituting for L_m, Eq. (42), we obtain a relationship between the minimum mass flux and external radiation.

$$\dot{m}''_F \left\{ c_p(T_{f,crit} - T_\infty)(1 + \frac{r}{Y_{ox,\infty}}) + L - \Delta h_c - c_p(T_v - T_\infty) \right\} = \dot{q}''_e - \sigma(T_v^4 - T_\infty^4) \tag{43}$$

From Eqs. (30) and (33)

$$\dot{m}''_F L = \frac{h_c}{c_p}\left(\frac{Y_{ox,\infty}\Delta h_c}{r} - c_p(T_v - T_\infty) \right) + \dot{q}''_e - \sigma(T_v^4 - T_\infty^4). \tag{44}$$

Subtracting Eq. (43) from Eq. (44) gives the minimum mass flux as

$$\dot{m}''_{o,b} = \frac{\left(\frac{h_c}{c_p}\right)\left[\frac{Y_{ox,\infty}\Delta h_c}{r} - c_p(T_v - T_\infty)\right]}{\Delta h_c + c_p(T_v - T_\infty) - c_p(T_{f,crit} - T_\infty)(1 + \frac{r}{Y_{ox,\infty}})} \tag{45}$$

An approximate expression can be found that is more revealing. Neglect $c_p(T_v - T_\infty)$, and recognize $r/Y_{ox,\infty}$ is typically much larger than 1. Then,

$$\dot{m}''_{o,b} \approx \frac{\left(\frac{h_c}{c_p}\right)\left(\frac{Y_{ox,\infty}}{r}\right)\Delta h_c}{\Delta h_c - c_p(T_{f,crit} - T_\infty)(\frac{r}{Y_{ox,\infty}})},$$

or
$$\dot{m}''_{o,b} \approx \frac{\left(\frac{h_c}{c_p}\right)\left(\frac{Y_{ox,\infty}}{r}\right)}{1 - \frac{c_p(T_{f,crit} - T_\infty)}{\frac{Y_{ox,\infty}\Delta h_c}{r}}} = \frac{\left(\frac{h_c}{c_p}\right)Y_{ox,\infty}\Delta h_{ox}}{\Delta h_c\left[1 - \frac{c_p(T_{f,crit} - T_\infty)}{Y_{ox,\infty}\Delta h_{ox}}\right]} \quad (46)$$

It can be shown that this critical flux relates to that for ignition using Eq. (23) as

$$\frac{c_p\dot{m}''_{o,b}}{h_c} \approx \frac{\left(\frac{Y_{ox,\infty}}{r}\right)^2}{\frac{Y_{ox,\infty}}{r} - \left(\frac{c_p\dot{m}''_{o,ig}}{h_c}\right)}. \quad (47)$$

This shows the approximate relationship between the mass flux for burning and that required for ignition. The role of $Y_{ox,\infty}$ is significant, along with convection.

Implicit in the comparison between the critical mass flux for ignition and extinction is that the critical flame temperature corresponding to the adiabatic flame temperature for the LFL mixture is the same as that at extinction. Macek in Reference [7] reported for alkanes that the computed adiabatic flame temperatures for complete combustion in air were about 1200-1400 °C at the **LFL** and roughly 1400-1500 °C at extinction in the limiting oxygen index test. In general, there appears to be sufficient experimental evidence to use about 1300 °C for both ignition and extinction in air. This critical temperature is related to the chemical kinetics behavior of the gaseous fuel, and more completely corresponds to a critical **E/RT** value. A single critical flame temperature is used throughout this analysis for these reasons.

1.4.6 Critical External Heat Flux at Extinction

The combination of Eqs. (42) and (43) showed the critical mass flux is a function of ambient condition, specifically oxygen concentration. Alternatively, eliminating the mass flux between Eqs. (42) and (43) will give a relationship between the external heat flux and the ambient conditions at extinction. Intuitively, it might be accepted that increasing the external heat flux,

ambient temperature, or oxygen concentration will make the flame harder to extinguish. Alternatively, increasing the heating by raising $\mathbf{T}_\infty$ or $\dot{\mathbf{q}}''_{\mathbf{e}}$ might allow burning to occur at lower oxygen concentrations. This has been shown, and is demonstrated by combining Eqs. (43) and (44) as [7]

$$\frac{\left(\frac{\mathbf{h_c}}{\mathbf{c_p}}\right)\left[\frac{\mathbf{Y_{ox,\infty}\Delta h_c}}{\mathbf{r}}-\mathbf{c_p(T_v-T_\infty)}\right]\left(\frac{\mathbf{Y_{ox,\infty}}}{\mathbf{r}}\right)\mathbf{L}}{\left\{\left(\frac{\mathbf{Y_{ox,\infty}}}{\mathbf{r}}\right)\left[\mathbf{\Delta h_c+c_p(T_v-T_\infty)}\right]-\left(\frac{\mathbf{Y_{ox,\infty}}}{\mathbf{r}}+\mathbf{1}\right)\mathbf{c_p(T_{f,crit}-T_\infty)}\right\}}$$

$$=\frac{\mathbf{h_c}}{\mathbf{c_p}}\left(\frac{\mathbf{Y_{ox,\infty}\Delta h_c}}{\mathbf{r}}-\mathbf{c_p(T_v-T_\infty)}\right)+\dot{\mathbf{q}}''_{\mathbf{e}}-\boldsymbol{\sigma}\mathbf{(T_v^4-T_\infty^4)} \tag{48}$$

Recognizing that $\mathbf{c_p\ (T_v - T_\infty)}$ **is** relatively small and $\mathbf{Y_{ox}/r} << 1$, then we can approximate the critical heat flux at extinction as

$$\dot{\mathbf{q}}''_{\mathbf{o,b}}\approx\boldsymbol{\sigma}\mathbf{(T_v^4-T_\infty^4)}-\left(\frac{\mathbf{h_c}}{\mathbf{c_p}}\right)\mathbf{Y_{ox,\infty}}\left(\frac{\mathbf{\Delta h_c}}{\mathbf{r}}\right)+\frac{\left(\frac{\mathbf{h_c}}{\mathbf{c_p}}\right)\frac{\mathbf{Y_{ox,\infty}^2}}{\mathbf{r}}\left(\frac{\mathbf{\Delta h_c}}{\mathbf{r}}\right)\mathbf{L}}{\mathbf{Y_{ox,\infty}}\left(\frac{\mathbf{\Delta h_c}}{\mathbf{r}}\right)-\mathbf{c_p(T_{f,crit}-T_\infty)}} \tag{49}$$

Since $\mathbf{r = \Delta h_c / \Delta h_{ox}}$,

$$\dot{\mathbf{q}}''_{\mathbf{o,b}}\approx\boldsymbol{\sigma}\mathbf{(T_v^4-T_\infty^4)}-\left(\frac{\mathbf{h_c}}{\mathbf{c_p}}\right)\mathbf{Y_{ox,\infty}\Delta h_{ox}}+\frac{\left(\frac{\mathbf{h_c}}{\mathbf{c_p}}\right)\mathbf{Y_{ox,\infty}\Delta h_{ox}}}{\left[\mathbf{1}-\frac{\mathbf{c_p(T_{f,crit}-T_\infty)}}{\mathbf{Y_{ox,\infty}\Delta h_{ox}}}\right]}\left(\frac{\mathbf{L}}{\mathbf{\Delta h_c}}\right) \tag{50}$$

This can be expressed in terms of the critical mass flux for extinction, and the critical heat flux for ignition from Eq. (46). Recognizing that

$$\boldsymbol{\sigma}\mathbf{(T_v^4-T_\infty^4)}\approx\ \boldsymbol{\sigma}\mathbf{(T_{ig}^4-T_\infty^4)}+\mathbf{h_c\,(T_{ig}-T_\infty)}\equiv\dot{\mathbf{q}}''_{\mathbf{o,ig}} \tag{51}$$

as $\mathbf{T_v}$ is only slightly higher than $\mathbf{T_{ig}}$ (Table 1-1). Then,

$$\dot{\mathbf{q}}''_{\mathbf{o,b}}\approx\dot{\mathbf{q}}''_{\mathbf{o,ig}}+\dot{\mathbf{m}}''_{\mathbf{b,o}}\mathbf{L}-\left(\frac{\mathbf{\Delta h_c}}{\mathbf{c_p}}\right)\mathbf{Y_{ox,\infty}\Delta h_{ox}}\,. \tag{52}$$

The last term is the heat flux from the flame at this oxygen mass fraction from Eq. (33). Physically, this says that the incident flame and external heat flux must be greater than the re-

radiation heat loss and the critical energy to vaporize the material. Alternatively, the sufficient net incident heat flux must produce more mass flux than the critical value by Eq. (46). From Eq. (50), the critical heat flux deceases with $\Delta h_c/L$ for a given ambient oxygen concentration.

1.4.7 Critical Mass Flux Estimates

Let us return to the critical mass fluxes for ignition and burning. Use values: $T_{f,crit} = 1300$ °C, $T_\infty = 25$ °C, and $c_p = 10^{-3}$ kJ/g-K. Let $h_c = 10$ W/m^{2}K, then

$$\dot{m}''_{o,ig} = h_c \frac{(T_{f,crit} - T_\infty)}{\Delta h_c} = (10x10^{-3})[(1300\text{-}25)/\Delta h_c].$$

Then the critical flux for ignition is

$$\dot{m}''_{o,ig} = \frac{12.8(kJ/m^2s)}{\Delta h_c}, \text{ in g/m}^2\text{s}. \tag{53}$$

For typical fuels, $\dot{m}''_{o,ig} \approx$ 0.28 to 1 g/m^{2}s, the critical mass flux for ignition increases with decreasing Δh_c i.e. liquids have lower values than charring solids. The critical mass flux for burning is estimated from Eq. (41) for burning in air. Let $\frac{\Delta h_c}{r}$ =13.1 kJ/g and $Y_{ox,\infty} = 0.233$, then

$$\dot{m}''_{o,b} \approx \left(\frac{10}{1}\right) \frac{\left(\frac{0.233}{r}\right)}{1 - \frac{10^{-3}(1300-25)}{0.233(13.1)}} \approx \frac{\frac{0.233}{r}}{1 - 0.4177}$$

or $$\dot{m}''_{o,b} \approx 4.0/r \text{ (g/m}^2\text{s)}.$$

Since $r = \frac{\Delta h_c}{\Delta h_{ox}}$, $$\dot{m}''_{o,b} \approx \frac{4.0\Delta h_{ox}}{\Delta h_c} = \frac{52.4\left(\frac{kJ}{gm^2s}\right)}{\Delta h_c} \tag{54}$$

Consequently, $\dot{m}''_{o,b} > \dot{m}''_{o,ig}$ for burning in air and ranges from about 1.2 to 4.4 g/m^{2}s for liquids and charring solids, respectively.

1.5 FLAME SPREAD

Consider flame spread as a succession of continuous ignitions. The speed (**v**) is considered steady (or quasi-steady) and is derived from the movement over a heated length, δ_f, raising the temperature from T_o to T_{ig} in time t_{ig}. The ignition time is estimated for the net incident flame heat flux, assumed uniform over δ_f. The surface flame speed is then simply,

$$v = \delta_f / t_{ig} \tag{55}$$

Over the flame heating length both the flame and external heat fluxes apply and the heat transfer coefficient is only due to re-radiation. From the heating equation for think and thin materials, and using the small time solutions due to expected height flame heat fluxes during spread, the time to ignite can be obtained from Eqs. (12) and (13)

$$\text{Thin: } T_{ig} - T_o = \left[\frac{\dot{q}''}{h_r} - (T_o - T_\infty)\right]\left(\frac{h_r t_{ig}}{\rho c \delta}\right) \tag{56a}$$

$$\text{Thick: } T_{ig} - T_o = \left[\frac{\dot{q}''}{h_r} - (T_o - T_\infty)\right]\left(\frac{4h_r^2 t_{ig}}{k\rho c}\right)^{1/2} \tag{56b}$$

where $\dot{q}'' = \dot{q}_f'' + \dot{q}_e''$ is the total incident heat flux. Furthermore, the pre-heating of the material can be described as

$$T_o - T_\infty = \left(\frac{\dot{q}_e''}{h_r + h_c}\right) F(t) . \tag{57}$$

where **F(t)** is given by Eq. (17), and here $h_t = h_r + h_c$. Substituting for the pre-heating in terms of the external radiative heat flux gives

$$\text{Thin: } t_{ig} = \frac{\rho c \delta\left[(T_{ig} - T_o) - \left(\frac{\dot{q}_e''}{h_r}\right)\beta F(t)\right]}{\dot{q}_f'' - \dot{q}_e''[1 - \beta F(t)]} \tag{58a}$$

$$\text{Thick: } t_{ig} = \frac{\pi}{4} k\rho c \left[\frac{(T_{ig} - T_\infty) - \frac{\dot{q}_e''}{h_r}\beta F(t)}{\dot{q}_f'' - \dot{q}_e''[1 - \beta F(t)]}\right]^2 \tag{58b}$$

where $\beta \equiv \dfrac{h_r}{h_r + h_c}$.

For long-time pre-heating **F(t)** = 1, and in general $\beta \approx 1$ since convection is relatively small. Then

Thin: $$t_{ig} = \frac{\rho c \delta (T_{ig} - T_o)}{\dot{q}''_f} \tag{59a}$$

Thick: $$t_{ig} = \frac{\pi}{4} k \rho c \left(\frac{(T_{ig} - T_o)}{\dot{q}''_f} \right)^2 \tag{59b}$$

Figures 1-18a and 1-18b show conditions for flame spread against (opposed) and wind-adided flow u_∞. Since the flame is moving at speed **v**, the relative wind speed is shown accordingly.

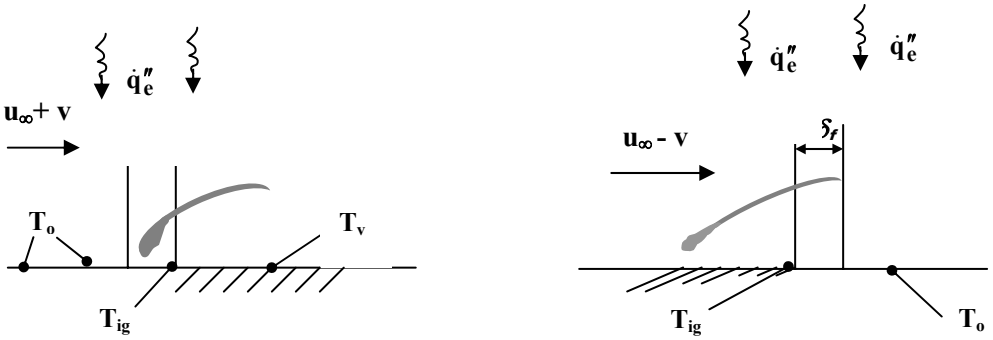

a) Opposed Flow b) Wind-aided

Figure 1-18. Representations of opposed and wind-aided flame spread.

1.5.1 Opposed Flow Spread Velocity

deRis [10] has derived exact solutions for the opposed flow case. They correspond to the thin and thick approximate solutions given here in terms of $\dot{q}''_f$ and δ_f. The diffusive length, δ_f, can be expressed in terms of the diffusivity as $\alpha_g/(u+v)$ where $\alpha_g = (k/\rho c)_g$. (The subscript **g** denotes gas.) The approximate and exact solutions correspond with

Thin:

$$\dot{q}''_f \delta_f = \sqrt{2} k_g (T_f - T_{ig}), \text{ giving } v = \frac{\sqrt{2} k_g (T_f - T_{ig})}{\rho c \delta (T_{ig} - T_o)} \tag{60a}$$

Thick:

$$(\dot{q}_f'')^2 \delta_f = \frac{\pi}{4}(k\rho c)_g (u_\infty + v)(T_f - T_{ig})^2 \text{ and } v = \frac{(k\rho c)_g (u_\infty + v)}{k\rho c} \frac{(T_f - T_{ig})^2}{(T_{ig} - T_o)^2} \quad (60b)$$

1.5.2 Conditions Needed for Opposed Flow Spread

Two criteria are considered for the cessation of opposed flow flame spread.

1. The leading edge of the flame is laminar and pre-mixed. The burning speed must be $u_\infty + v$. For its propagation to be sustained, the mass flux near the leading edge must produce the lower flammable limit. This is the **LFL** criterion for opposed flow spread.
2. The incident heat flux from the flame and the external radiant flux must exceed the critical flux for ignition. If this criterion is not met, the flame will cease to propagate.

1.6 FLAMMABILITY LIMIT

1.6.1 Criterion 1: Lower Flammability Limit

Here the fuel mass flux needed to achieve the lower flammable limit must match the mass flux produced by heating. This process is portrayed in Figure 1-19. From Eq. (19) the LFL mass flux is

$$\dot{m}_F'' = \frac{h_c (T_{f,crit} - T_o)}{\Delta h_c} \quad (61)$$

The mass flux due to heating is represented by either Eq. (39) or (47) where the flame convective heat flux is represented at this critical flame temperature:

$$\dot{m}_F'' = \frac{h_c (T_{f,crit} - T_o) + \dot{q}_e'' - \sigma(T_{ig}^4 - T_\infty^4)}{L} \quad (62)$$

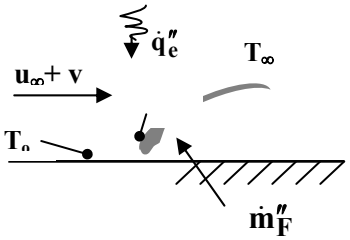

Figure 1-19 Mass flux at the flame tip.

Equating these two equations will give the critical conditions in terms of T_o and $\dot{q}''_e$. Recall for long time heating, with the initial and ambient temperature at T_∞:

$$T_o - T_\infty = \frac{\dot{q}''_e}{h_t}. \tag{63}$$

where, $h_t = h_r + h_c$. Then equating yields:

$$\frac{h_c\left[(T_{f,crit} - T_\infty) - (T_o - T_\infty)\right]}{\Delta h_c} = \frac{h_c(T_{f,crit} - T_\infty) + h_t(T_o - T_\infty) - \sigma(T_{ig}^4 - T_\infty^4)}{L}$$

Rearranging,

$$\left(\frac{h_t}{L} + \frac{h_c}{\Delta h_c}\right)(T_o - T_\infty) =$$

$$\frac{h_c(T_{f,crit} - T_\infty)}{\Delta h_c} + \frac{\sigma(T_{ig}^4 - T_\infty^4)}{L} - \left\{\frac{h_c(T_{f,crit} - T_\infty)}{L} - \frac{h_c}{L}(T_{ig} - T_\infty)\right\}$$

$$= h_c(T_{f,crit} - T_\infty)\left(\frac{1}{\Delta h_c} - \frac{1}{L}\right) + \frac{h_t(T_{ig} - T_\infty)}{L}$$

This is for long-time heating, where the applied radiant heat flux is uniquely related to the pre-heated surface temperature, the equation gives the minimum surface temperature for opposed flow flame spread, $T_{o,s}$

$$T_{o,s} - T_\infty = \frac{\frac{h_t}{h_c}\left(\frac{\Delta h_c}{L}\right)(T_{ig} - T_\infty) - \left(\frac{\Delta h_c}{L} - 1\right)(T_{f,crit} - T_\infty)}{\frac{h_t}{h_c}\left(\frac{\Delta h_c}{L}\right) + 1} \tag{64}$$

Alternatively, this can be written in terms of the critical heat flux for spread, and recognizing that $\dot{q}''_{o,ig} = h(T_{ig} - T_\infty)$ is the critical heat flux for ignition, the critical heat flux for Criterion 1 is

$$\left(\dot{q}''_{o,s}\right)_1 = \frac{\frac{h_t}{h_c}\left(\frac{\Delta h_c}{L}\right)\dot{q}''_{o,ig} - \left(\frac{\Delta h_c}{L} - 1\right)(T_{f,crit} - T_\infty)}{\frac{h_t}{h_c}\left(\frac{\Delta h_c}{L}\right) + 1} \tag{65}$$

The importance of the $\mathbf{HRP} = \Delta h_c/L$ and the convective heat transfer coefficient is evident.

1.6.2 Criterion 2: Critical Heat Flux for Ignition

At the flame heating region, the critical heat flux must be achieved or no ignition and therefore no spread will occur. This condition requires from Eq. (5) for either thick or thin materials that

$$\dot{q}''_f + \dot{q}''_e = \sigma(T_{ig}^4 - T_\infty^4) = h_r (T_{ig} - T_\infty) \tag{66}$$

Let us make some estimates of $\dot{q}''_e = \left(\dot{q}''_{o,s}\right)_2$. For opposed flow spread in air, $\dot{q}''_f \approx$ 50-70 (kW/m^2) from measurements in the literature [11]. Alternatively, for laminar flow flame temperatures in air, $T_f \approx 2000$ °C, and we can estimate this flame incident heat flux as

$$\dot{q}''_f = h_{c,f} (T_f - T_{ig}) \approx 50 \text{ W/m}^2\text{-K x } 10^{-3} \text{ kW/W x (2000-500 K)} \approx 75 \text{ (kW/m}^2\text{)} \tag{67}$$

This estimate is consistent with measurements, and suggests Eq. (67) as a valid representation of the flame incident heat flux. Estimating $\sigma(T_{ig}^4 - T_\infty^4)$ for typical ignition temperatures e.g. $T_{ig} \approx$ 500 °C, gives $\sigma(T_{ig}^4 - T_\infty^4) \approx 20$ (kW/m^2). Hence, representing the critical heat flux as

$$\left(\dot{q}''_{o,s}\right)_2 = \sigma(T_{ig}^4 - T_\infty^4) - h_{c,f} (T_f - T_\infty), \tag{68}$$

that indicates that this critical heat flux is always negative. Hence, critical heat flux does not likely control spread.

1.6.3 Controlling Criterion for Opposed Flow Spread

Let us examine these two criteria and compare them with some approximations. From Criterion 1, Eq. (66), since the first term in the denominator is larger than 1,

$$\left(\dot{q}''_{o,s}\right)_1 \approx \dot{q}''_{o,ig} - h_c \left(1 - \frac{L}{\Delta h_c}\right)(T_{f,crit} - T_\infty) \tag{69}$$

This compares to the approximate Criterion 2 as

$$\left(\dot{q}''_{o,s}\right)_2 \approx \dot{q}''_{o,ig} - h_{c,f} (T_f - T_\infty). \tag{70}$$

In general, $h_{c,f} (T_f - T_\infty) > h_c (1 - L / \Delta h_c)(T_{f,crit} - T_\infty)$ and therefore,

$$\left(\dot{q}''_{o,s}\right)_1 > \left(\dot{q}''_{o,s}\right)_2. \tag{71}$$

Hence, Criterion 1 clearly controls the spread process.

1.6.4 Wind-aided or Upward Flame Spread Characteristics

We will consider upward flame spread by natural convection. The flame may be laminar or turbulent. The process is depicted in Figure 1-20.

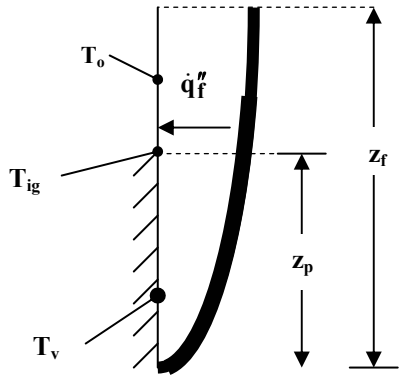

Figure 1-20 Upward flame spread in terms of z_p, the pyrolysis length, and z_f, the flame length.

For tests using small flame ignition sources, such as FMVSS 302, upward flame spread would be initiated as a laminar flame. For a larger flame ignition source or radiant induced ignition over a relatively large region (height > 0.3 m), the initial flame spread will be turbulent. The behavior of laminar and turbulent flame heat fluxes and their lengths will control the process. Turbulent wall flames of moderate size (height ~ 1-2 m) will impart an incident heat flux of roughly 20-30 kW/m^2. Laminar heat fluxes could be double this due to hotter flames that are closer to the wall. In both cases the length of the flames depend on the energy release rate per unit width, $\dot{Q}' = \dot{Q} / w$. The width, **w**, is the lateral wall dimension over which the flame is spreading. In terms of the pyrolysis or vaporization region, z_p,

$$\dot{Q}' = \dot{Q}'' z_p . \tag{72}$$

Thus the fire energy flux or rate of heat release per unit area is a factor affecting the flame length. In contrast to the opposed flow case, the flame heated length to initiate ignition is no longer constant as the spread ensues. Here

$$\delta_f = z_f - z_p \tag{73}$$

where z_f depends on $\dot{Q}''z_p$. Thus, the energy flux of a material is a critical factor in controlling wind-aided spread. Although this factor did not enter into the results for opposed flow spread, its underlying property parameter $\Delta h_c/L$ did. Hence, we see that functionally

$$\delta_f = f\left(\frac{\Delta h_c}{L}\right). \tag{74}$$

1.6.5 Upward Wall Flame Length

It can be shown [11] that wall flame lengths can be expressed as a power relationship for $\dot{Q}'$ by

$$z_f = a\left(\dot{Q}'\right)^n \tag{75}$$

Results are shown from Ahmed and Faeth in Quintiere [11] for turbulent flames, ($n = ⅔$)

$$z_f = \frac{1.02 l_c}{Y_{ox,\infty}(1 - X_r)^{\frac{1}{3}}} \tag{76}$$

where $l_c = \left(\frac{\dot{Q}'}{\rho_\infty c_p T_\infty \sqrt{g}}\right)^{\frac{2}{3}}$ is a characteristic plume length.

For laminar flames ($n = 2$):

$$z_f = 0.023 \frac{r^{\frac{7}{3}}}{\left(Y_{ox,\infty}\right)^{\frac{1}{3}}} \frac{l_c^2}{l_v} \tag{77}$$

$l_v = \left(\frac{\mu}{\frac{\rho}{\sqrt{g}}}\right)^{\frac{2}{3}}$, is a viscous length.

Sometimes a linear approximation is made for the turbulent case that dramatically shows that upward turbulent flame spread can either accelerate or decelerate to extinction. That approximation for n = 1, gives a = 0.01 m^2/kW. This compares to a = 0.0436 (m^2/kW)^{⅔} for n = ⅔ in air. If $\dot{Q}'$ = 100 kW/m^2, then z_f = 1 m for n = 1, and z_f = 0.97 m for n = ⅔.

1.6.6 Upward Flame Spread

Consider flame spread under external radiant heating such that this external heating preheats the material and enhances its burning rate. For simplicity, the radiant heating will be considered to have acted for a long-time. Steady burning and pre-heating to a unique temperature, $\mathbf{T_o}$, occurs under this heat flux, $\dot{\mathbf{q}}''_{\mathbf{e}}$. The upward flame spread speed is not necessarily constant as

$$\mathbf{v} = \frac{\mathbf{dz_p}}{\mathbf{dt}} = \frac{\delta_\mathbf{f}}{\mathbf{t_{ig}}} \tag{78}$$

The ignition time is constant and given as in the long-time pre-heated opposed flow case. Substituting for the flame heated length gives

$$\frac{\mathbf{dz_p}}{\mathbf{dt}} = \frac{\mathbf{a}\left(\dot{\mathbf{Q}}''\mathbf{z_p}\right)^{\mathbf{n}} - \mathbf{z_p}}{\mathbf{t_{ig}}} \tag{79}$$

Let

$$\mathbf{k_f} = \mathbf{a}\left(\dot{\mathbf{Q}}''\right)^{\mathbf{n}} \mathbf{z_{p,o}^{n-1}}\mathbf{;\ t = 0,\ z_p = z_{p,o}\ ,\ x = z_p / z_{p,o}\ and\ \tau = t / t_{ig}} \tag{80}$$

Then

$$\frac{\mathbf{dx}}{\mathbf{d\tau}} = \mathbf{k_f x^n - x} \tag{81}$$

The dimensionless parameter $\mathbf{k_f}$ controls whether the flame accelerates or stops. Here we see $\mathbf{k_f}$ depends again on the $\mathbf{HRP} = \Delta\mathbf{h_c/L}$ of the material and on the extent of the ignited region, $\mathbf{z_{p,o}}$. Explicitly for $\mathbf{k_f << 1,}$ or small $\dot{\mathbf{Q}}$ and small $\mathbf{z_{p,o}}$,

$$\mathbf{z_p = z_{p,o} e^{-\left(t/t_{ig}\right)}} \tag{82}$$

and the flame cannot advance. This is why in tests with small ignition sources, if $\Delta\mathbf{h_c/L}$ is not large enough, the flame may not propagate. A different result can occur for a larger ignited region. As for $\mathbf{k_f > 1,}$ we approximate, neglecting the *x* term

$$\int_{\mathbf{x(0)}}^{\mathbf{x}} \frac{\mathbf{dx}}{\mathbf{x^n}} = \mathbf{k_f \tau} \tag{83}$$

$$n \neq 1 \quad \mathbf{z_p = z_{p,o}}\left[\mathbf{1 + (1 - n) k_f}\ t/\mathbf{t_{ig}}\right]^{\frac{\mathbf{1}}{\mathbf{1-n}}} \tag{84a}$$

$$\mathbf{n = 1 \quad z_p = z_{p,o} e^{k_f t / t_{ig}}} \tag{84b}$$

Turbulent, $\mathbf{n = \frac{2}{3}}$

$$\mathbf{z_p = z_{p,o}\left[1 + \frac{k_f t}{3 t_{ig}}\right]^3} \tag{84c}$$

Laminar, $\mathbf{n = 2}$

$$\mathbf{z_p = z_{p,o}\left[1 - k_f t / t_{ig}\right]^{-1}} \tag{84d}$$

In all cases of **n** values, the flame accelerates.

1.6.7 Conditions Necessary for Upward Flame Spread

Here three criteria are considered for upward flame spread.

1. The flame length is too short, i.e. $z_f = z_p$ at the limit of $v = 0$, where the flame stops.
2. The heat flux from the flame and external heat sources must be greater than the critical flux for ignition. This is the same as Criterion 2 in opposed flow spread, but the flame heat flux is different in upward spread.
3. The material burns out before ignition of a new element can occur. The burn-out time is given from the burning rate and mass of material available.

Criterion 1: Flame Length

From the flame spread equation the flame will stop ($\mathbf{v} = 0$) when $\mathbf{z_f = z_p}$. This criterion is expressed from Eq. (75) by

$$\mathbf{z_p = a\left(\dot{Q}'' z_p\right)^n} \tag{85}$$

and the maximum distance that can occur is

$$\mathbf{z_{p,max} = \left[a \dot{Q}''^n\right]^{\frac{1}{1-n}}}. \tag{86}$$

For the laminar case,

$$\mathbf{z_{p,max} \sim \dot{Q}''^{-2} \sim (\Delta h_c / L)^{-2}} \tag{87}$$

However, this result is somewhat pathological as it will only hold up to about $\mathbf{z_{p,max} \sim 0.3}$ m where the flame will become turbulent. It suggests that materials with small $\mathbf{\Delta h_c/L}$ take longer to become turbulent. For the more important and relevant turbulent case, for $\mathbf{n = \frac{2}{3}}$,

$$\mathbf{z_{p,max} = \left[0.0436 \left(\frac{m^2}{kW} \right)^{2/3} \dot{Q}''^{2/3} \right]^3}$$

or $$\mathbf{z_{p,max} = 8.29 x 10^{-5} \dot{Q}''^2} \tag{88}$$

For $\dot{Q}''$ = 100 kW/m^2, this says $z_{p,max}$ = 0.83 m, or for $\dot{Q}''$ = 50 kW/m^2 the flame vaporization zone will only move to 0.21 m at most. If the ignition source exceeds this maximum propagation length, no spread will occur. Hence, for "large" ignition sources, say 0.3 m, turbulent spread will not occur for $\dot{Q}''$ less than 50-100 kW/m^2.

If we had examined this case for the approximate flame length formula with n = 1, it would give

$$\mathbf{0.01 (m^2/kW) \dot{Q}'' = 1}$$

for all cases. Hence, both of these results for the turbulent case ($\mathbf{n = 2/3 - 1}$) indicate a critical energy flux as

$$\mathbf{\dot{Q}''_{o,s} \approx 50 \text{ to } 100 \text{ kW/m}^2.} \tag{89}$$

The corresponding fuel mass flux is

$$\mathbf{\dot{m}''_{o,s} = \frac{\dot{Q}''_{o,s}}{L}}. \tag{90}$$

The corresponding critical radiant heat flux for upward spread under this criterion is given from Eq. (39) in terms of the flame incident heat flux as

$$\mathbf{\dot{q}''_f + \dot{q}''_e - \sigma (T_v^4 - T_\infty^4) = \dot{Q}''_{o,s} \left(L / \Delta h_c \right)}. \tag{91}$$

Hence, the limiting external heat flux is

$$\mathbf{\left(\dot{q}''_{o,s} \right)_1 = \sigma (T_v^4 - T_\infty^4) - h_f (T_f - T_\infty) + \dot{Q}''_{o,s} \left(L / \Delta h_c \right)} \tag{92}$$

where the incident flame heat flux has been expressed in terms of a turbulent flame temperature and an overall heat transfer coefficient, $\mathbf{h_f}$. The form of this critical external flux can be compared to that controlling opposed flow flame spread, i.e.

$$\left(\dot{q}''_{o,s}\right)_{1,\mathbf{opposed}} \approx \dot{q}''_{o,ig} - h_c\left(1 - \frac{L}{\Delta h_c}\right)(T_{f,crit} - T_\infty)\,. \tag{93}$$

The first two terms in each expression can be argued to have similar magnitudes, and therefore it might be approximated that

$$\left[\dot{q}''_{o,s}\right]_{\mathbf{upward}} \approx \left[\dot{q}''_{o,s}\right]_{\mathbf{opposed}} + \dot{Q}''_{o,s}\left(L/\Delta h_c\right). \tag{94}$$

Considering estimates for the results of Criterion 2 by Eq. (88), the incident flame heat flux to the surface is generally about 30 kW/m^2 [11]; for melting materials: $T_v \approx 350$ °C and $L/\Delta h_c = 0.1$, and for charring materials: $T_v \approx 450$ °C and $L/\Delta h_c = 1$. It follows that the critical flux for upward spread under Criterion 2 is roughly

$\left(\dot{q}''_{o,s}\right)_1 \approx -10$ kW/m^2 for melting materials,

$\left(\dot{q}''_{o,s}\right)_1 \approx 85$ kW/m^2 for charring materials.

These are only extreme estimates and general results for materials fall in between. In general, this critical heat flux depends strongly on the last term or $L/\Delta h_c$. It decreases as $L/\Delta h_c$ decreases, or **HRP** increases.

Criterion 2: Critical Heat Flux

This criterion is the same as that applied to opposed flow spread, but the flame incident heat flux is lower here by about a factor of 2. Representing the turbulent flame incident heat flux as in Criterion 1 gives

$$\left(\dot{q}''_{o,s}\right)_2 = \sigma(T_{ig}^4 - T_\infty^4) - h_f(T_f - T_\infty) \tag{95}$$

Here h_f implies convective and radiative effects. As before, approximate this as

$$\left(\dot{q}''_{o,s}\right)_2 \approx \dot{q}''_{o,ig} - h_f(T_f - T_\infty) \tag{96}$$

Comparing the two criteria, gives

$$\left(\dot{q}''_{o,s}\right)_1 \approx \left(\dot{q}''_{o,s}\right)_2 + \dot{Q}''_{o,s}\left(L/\Delta h_c\right), \tag{97}$$

and it shows that Criterion 1 controls over Criterion 2.

Criterion 3: Burnout

If the material burns to extinction before ignition can occur to the next material element for spread, spread will cease. This condition occurs when the ignition time for flame spread is equal to the burning time, $\mathbf{t_b}$. As before, we consider steady burning and *long-time heating* by the external heat flux. From our introduction to flame spread, $\mathbf{t_{ig}}$ under these long-time conditions is given approximately by Eq. (58) as

Thin: $$\mathbf{t_{ig} = \frac{\rho c \delta \left[(T_{ig} - T_\infty) - \frac{\dot{q}''_e}{h_t} \right]}{\dot{q}''_f}} \tag{98a}$$

Thick: $$\mathbf{t_{ig} = \frac{\pi}{4} k \rho c \left[\frac{(T_{ig} - T_\infty) - \frac{\dot{q}''_e}{h_t}}{\dot{q}''_f} \right]}. \tag{98b}$$

Under steady burning,

$$\mathbf{\dot{m}''_F t_b = \rho \delta} \tag{99}$$

where recall Eq. (30)

$$\mathbf{\dot{m}''_F L = \dot{q}''_f + \dot{q}''_e - \sigma\left(T_v^4 - T_\infty^4\right)}$$

Equating these terms gives the following:

Thin: $$\mathbf{\frac{\rho \delta L}{\dot{q}''_f + \dot{q}''_e - \sigma\left(T_v^4 - T_\infty^4\right)} = \frac{\rho c \delta \left[(T_{ig} - T_\infty) - \dot{q}''_e / h_t \right]}{\dot{q}''_f}} \tag{100}$$

Rearranging and introducing the critical flux for ignition gives

$$\mathbf{\frac{L}{c(T_{ig} - T_\infty)} = \left(1 - \frac{\dot{q}''_e}{\dot{q}''_{o,ig}}\right)\left(1 + \frac{\dot{q}''_e}{\dot{q}''_f} - \frac{\sigma(T_v^4 - T_\infty^4)}{\dot{q}''_f}\right)} \tag{101}$$

This is a non-linear equation so some approximations are in order to obtain an estimate for the critical flux. It can be argued that the second parenthesis on the right-hand-side is approximately 1 since the flame heat flux is usually much higher than the other fluxes. Then,

$$\mathbf{\frac{L}{c(T_{ig} - T_\infty)} \approx 1 - \frac{\dot{q}''_e}{\dot{q}''_{o,ig}}}, \tag{102}$$

from which,

$$\left(\dot{q}''_{o,s}\right)_3 \approx \dot{q}''_{o,ig}\left[1-\frac{L}{c(T_{ig}-T_\infty)}\right] \tag{103}$$

This result is extremely interesting as always $L > c\,(T_{ig} - T_\infty)$, implying that

$$\left(\dot{q}''_{o,s}\right)_{3,thin} < 0. \tag{104}$$

It says, this criterion is not relevant for thin materials, but it will be important for the thick case.

Thick:

Similarly for the thick case, we obtain by equating the burning time to the ignition time:

$$\frac{4}{\pi}\frac{\dot{q}''_{f,net}\delta}{kc(T_{ig}-T_\infty)^2}=\left(1-\frac{\dot{q}''_e}{\dot{q}''_{o,ig}}\right)^2\left(1+\frac{\dot{q}''_e}{\dot{q}''_f}-\frac{\sigma(T_v^4-T_\infty^4)}{\dot{q}''_f}\right) \tag{105}$$

Approximately, as before, gives

$$\left(\dot{q}''_{o,s}\right)_3 \approx \dot{q}''_{o,ig}\left[1-\left(\frac{\rho\delta\dot{q}''_f}{\frac{\pi}{4}(k\rho c)(T_{ig}-T_\infty)^2}\right)^{1/2}\right] \tag{106}$$

Tewarson's **TRP** enters here for the thick case. It is significant that the critical heat flux does not depend on thickness for the thin case, but does for the thick case. As the thickness approaches zero, the critical flux for spread approaches its upper limit equal to the critical flux for ignition. This says no flame spread is possible.

It is important to compare the results from Criteria 1 and 3 to see which one controls. Whichever critical flux is larger, it controls. Rewrite and approximate Eq. (92)

$$\left(\dot{q}''_{o,s}\right)_1 \approx \dot{q}''_{o,ig} - \dot{q}''_f + \dot{Q}''_{o,s}\left(L/\Delta h_c\right) \tag{107}$$

From Eq. (102) we see

$$\left(\dot{q}''_{o,s}\right)_3 \le \dot{q}''_{o,ig} \equiv CHF \tag{108}$$

and approaches the **CHF** when $\delta \to 0$. Conditionally, Eq. (107) must always hold for a relevant critical flux during flame spread, as the critical flux for spread cannot exceed **CHF** if flame spread is to exist. Hence, if

$$\left(\dot{q}''_{o,s}\right)_1 > CHF,$$

then Criterion 1 solely controls, and flame spread is not possible. This occurs if

$$\mathbf{HRP} \equiv \frac{\Delta h_c}{L} < \frac{\dot{Q}''_{o,s}}{\dot{q}''_f}.$$

Estimating the flame heat flux as 25 kW/m^2 and the critical energy flux term as ranging from 50 to 100 kW/m^2, indicates that this occurs when

$$\frac{\Delta h_c}{L} < \frac{\dot{Q}''_{o,s}}{\dot{q}''_f} \approx \frac{\mathbf{50 \text{ to } 100 \text{ kW/m}^2}}{\mathbf{20 \text{ to } 30 \text{ kW/m}^2}} \approx 2 \text{ to } 4.$$

For materials having relatively low $\Delta h_c/L$, which would correspond to charring materials for the most part, Criterion 1 would apply, and burnout may not be a factor, given the approximation made here. For materials, having higher $\Delta h_c/L$ values, either criterion could apply. It should be pointed out that these estimates are only for approximate indication purposes. Referring back to the more complete result for Criterion 1:

$$\left(\dot{q}''_{o,s}\right)_1 = \sigma(T_v^4 - T_\infty^4) - h_f(T_f - T_\infty) + \dot{Q}''_{o,s}\left(L/\Delta h_c\right)$$

for charring materials, the first term is not constant but increases as the surface temperature and accordingly the re-radiation term increases. Hence, a more precise estimate for charring or low $\Delta h_c/L$ materials is that the critical flux will be finite given its estimate as

$$\left(\dot{q}''_{o,s}\right)_1 \sim 15 - 25 + 100/(\Delta h_c/L) \text{ kW/m}^2$$

This can be positive when $\Delta h_c/L < 10$. Hence, this suggests that for other materials with $\Delta h_c/L$ large, either Criterion 1 or 3 can apply for thick materials.

1.7 FLAMMABILITY AND HEAT FLUX

Let us summarize these results for the case of long-time heating under an external radiant heat flux exposure. The processes of fire growth or a material's flammability can be decomposed into ignition, mass burning flux, energy flux (**HRR**), and flame spread. Flame spread has been distinguished between upward and opposed flow spread, and thick and thin materials are considered. Theoretical results have shown the relationships between burning rate, ignition and spread. In addition, the critical radiant heat flux associated with each process has been modeled. These critical fluxes give the lower or minimum heat flux where each process can occur. If the critical flux is positive, heat is needed to sustain the process. In deriving the relationships for the processes and their limiting fluxes, it has been seen that material properties emerge. Notably

they include Δh_c, L, T_{ig}, $k\rho c$ for thick, and $\rho c\delta$ for thin materials. These properties can be determined from fire testing procedures by approximate models and appropriate time averaging.

It is useful to recapitulate our results showing how the process variables plot with heat flux, and how some of these properties can be determined. In addition, it will be useful to relate these results to parameters identified and measured by Tewarson. Tewarson parameters are

$$\text{Thermal Response Parameter, } \mathbf{TRP} = \sqrt{\frac{\pi}{4}(k\rho c)}\left(T_{ig} - T_\infty\right)$$

$$\text{Critical Heat Flux, } \mathbf{CHF} = h(T_{ig} - T_\infty) \equiv \dot{q}''_{o,ig}$$

$$\text{Heat Release Parameter, } \mathbf{HRP} = \frac{\Delta h_c}{L}$$

$$\text{Flame Propagation Index, } \mathbf{FPI} \equiv 749\left(\dot{Q}'\right)^{1/3} / \mathbf{TRP}$$

In addition, as we have seen, critical heat fluxes for flame spread can be identified. In Tewarson's context, let us call these **CHFS**, *Critical Heat Flux for Spread*. As we recapitulate, we will show where these measurable Tewarson parameters apply along with the original property set.

1.8 BURNING RATE -- STEADY OR PEAK AVERAGE, $\dot{m}''_F\left(g/m^2 s\right)$

Burning flux as portrayed by Figure 1-13 is given by

$$\dot{m}''_F = \frac{\dot{q}''_f - \sigma(T_v^4 - T_\infty^4) + \dot{q}''_e}{L} \tag{109}$$

which holds for $\dot{q}''_e \geq \dot{q}''_{o,b}$ (Eq. (47)), the critical heat flux for burning:

$$\mathbf{CHFB} \equiv \dot{q}''_{o,b} \approx \dot{q}''_{o,ig} + \dot{m}''_{b,o} L - \left(\frac{h_c}{c_p}\right) Y_{ox,\infty} \Delta h_{ox}$$

with

$$\dot{m}''_{b,o} \approx \frac{\dfrac{h_c}{c_p} Y_{ox,\infty} \Delta h_{ox}}{\left[1 - \dfrac{c_p (T_{f,crit} - T_\infty)}{Y_{ox,\infty} \Delta h_{ox}}\right] \Delta h_c} \approx \frac{52.4}{\Delta h_c} \text{ in air. } \left(\Delta h_c \text{ in } \frac{kJ}{g}\right)$$

Thus, the ***Critical Heat Flux for Burning, CHFB, depends on CHF and HRP***.

1.9 HEAT RELEASE RATE OR ENERGY FLUX, $\dot{Q}''\left(kW/m^2\right)$

The energy flux can be expressed as

$$\dot{Q}'' = \dot{m}_F'' \Delta h_c, \left(\dot{q}_e'' \geq \dot{q}_{o,b}''\right) \tag{110}$$

It can also be plotted against the external heat flux and from the slope of the data, $\mathbf{HRP} = \frac{\Delta h_c}{L}$ can be found. Thus,

$$\dot{Q}'' \sim \mathbf{HRP}$$

1.10 IGNITION

For an initial temperature equal to the ambient, the time to ignite can be expressed as

$$t_{ig} = \text{ or } \begin{cases} \dfrac{\rho c \delta (T_{ig} - T_\infty)}{\dot{q}_e''}, \text{ Thin} \\ \dfrac{\pi}{4} k \rho c \left(\dfrac{T_{ig} - T_\infty}{\dot{q}_e''} \right)^2, \text{ Thick} \end{cases} \tag{111}$$

From plots of the ignition data as illustrated in Figures 1-21a and 1-21b, properties can be determined.

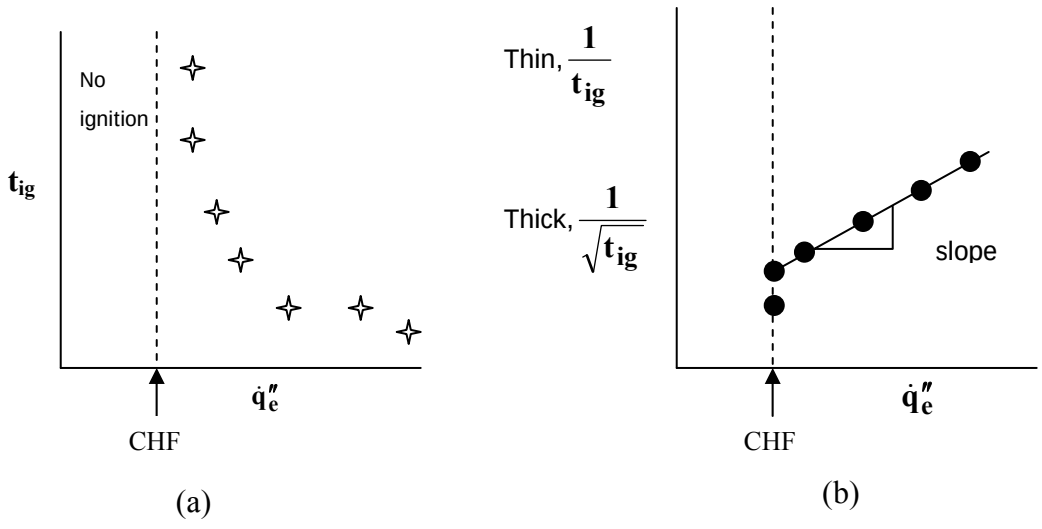

Figure 1-21 Ignition data and properties.

From the slope of $\mathbf{1/t_{ig}}$ (thin) or $\mathbf{1/t_{ig}^{½}}$ (thick) plotted against the heat flux the parameters $\mathbf{\rho c\delta(T_{ig}-T_\infty)}$ and $\mathbf{((\pi/4)k\rho c)^{½}\ (T_{ig}-T_\infty)}$ can be found. The latter is **TRP**. Hence, *for thick materials*

$$t_{ig} \sim (\mathbf{TRP})^2$$

These equations hold for $\mathbf{\dot{q}''_e \geq \dot{q}''_{o,ig}}$ where

$$\mathbf{\dot{q}''_{o,ig} = h_t (T_{ig} - T_\infty) = CHF.} \tag{112}$$

The piloted ignition temperature is essentially the flashpoint. Regard this critical flux as applying to piloted ignition; however, a set of data for auto-ignition could yield similar results. *The mass flux corresponding to piloted ignition is less than that at the extinction of burning* as taken from Eq. (23)

$$\mathbf{\dot{m}''_{o,ig} = \frac{h_{c,f}(T_{f,crit} - T_\infty)}{\Delta h_c} \approx \frac{12.8}{\Delta h_c} (g/m^2 s).\ (\Delta h_c \text{ in } \frac{kJ}{g})} \tag{113}$$

1.11 FLAME SPREAD

The flame spread velocity can be expressed as

$$\mathbf{v = \frac{\delta_f}{t_{ig}}} \tag{114}$$

where here the ignition time is given for a material pre-heated by a uniform external radiant heat flux for a long-time. For this case

$$\mathbf{t_{ig}} = \text{ or } \begin{cases} \dfrac{\rho c\delta\left[(T_{ig} - T_\infty) - \dot{q}''_e / h_t\right]}{\dot{q}''_f}, \text{ Thin} \\ \dfrac{\pi}{4} k\rho c \left[\dfrac{(T_{ig} - T_\infty) - \dot{q}''_e / h_t}{\dot{q}''_f}\right]^2, \text{ Thick} \end{cases} \tag{115}$$

1.11.1 Opposed Flow Spread

Exact solutions for opposed flow flame spread show

$$\delta_f = \quad \text{or} \quad \begin{cases} \sqrt{2}k_g / h_{c,f}\,, \text{ Thin} \\ \dfrac{\pi}{4}\dfrac{(k\rho c)_g (u_\infty + v)}{(h_{c,f})^2}\,, \text{ Thick} \end{cases} \tag{116}$$

from exact solutions, and representing the flame heat flux as

$$\dot{q}''_f = h_{c,f}(T_f - T_{ig}) \tag{117}$$

This shows δ_f is essentially constant under natural convection conditions since u_∞ will not change at the flame front.

This equation for spread rate holds for $\dot{q}''_e \geq \dot{q}''_{o,s}$. The controlling critical flux was found to be associated with maintaining the lower flammable limit at the flame front. From Eq. (69) the Critical Flux for flame Spread, Opposed is

$$\text{CHFSO} \equiv (\dot{q}''_{o,s})_1 \approx \dot{q}''_{o,ig} - h_c\left(1 - \frac{L}{\Delta h_c}\right)(T_{f,crit} - T_\infty)\,. \tag{118}$$

Thus we see in *opposed flow flame spread for thick materials*

$v \sim (\text{TRP})^{-2}$

and **CHFSO ~ CHF, HRP.**

1.11.2 Upward Spread

Upward spread is more complex. Equation (109) applies for flame speed; however, here δ_f depends on **HRP.** Hence,

$$v \sim \frac{(\text{HRP})^n}{(\text{TRP})^2}$$

For $n = ⅔$, as in turbulent wall flames,

$$v \sim \left[\frac{(\text{HRP})^{1/3}}{\text{TRP}}\right]^2 \sim (\text{FPI})^2$$

So approximately the *flame speed depends on Tewarson's FPI.* More specific results follow:

The parameter $\mathbf{k_f}$, which is dimensionless,

$$\mathbf{k_f \equiv a\ \left(\dot{Q}''\right)^n z_{p,o}^{n-1}}$$

controls the flame speed. Here **a** is a constant from the flame height relationship, and $\mathbf{z_{p,o}}$ is the initial height ignited. The power **n** can be 2 for laminar flames, and ⅔ to 1 for turbulent flames. The factor **a** has appropriate units. Dimensionless flame speed depends on $\mathbf{k_f}$ from Eq. (80) as

$$\frac{\mathbf{d}\left(\mathbf{z_p}/\mathbf{z_{p,o}}\right)}{\mathbf{d}\left(\mathbf{t}/\mathbf{t_{ig}}\right)} \sim \mathbf{k_f}$$

Therefore, the speed is given as

$$\mathbf{v} = \frac{\mathbf{dz_p}}{\mathbf{dt}} \sim \frac{\mathbf{k_f z_{p,o}}}{\mathbf{t_{ig}}} \text{ or } \mathbf{v} \sim \frac{\left(\dot{\mathbf{Q}}''\right)^{\mathbf{n}} \mathbf{z_{p,o}^n}}{\mathbf{t_{ig}}} \sim \frac{\left(\frac{\Delta \mathbf{h_c}}{\mathbf{L}}\right)^{\mathbf{n}} \left(\mathbf{z_{p,o}}\right)^{\mathbf{n}}}{\left(\mathbf{TRP}\right)^{\mathbf{2}}}. \tag{119}$$

Thus *flame speed depends on HRP, TRP, and ignition length*. It is clearly shown that in addition to material properties the upward speed depends on the extent of the material ignited. This may explain why small ignition sources may not lead to results expected in actual fires. The factors that control the critical external heat flux needed for upward flame spread depend on either flame length or burning time. The flame length criterion gives (Eq. (92) :

$$\mathbf{CHFSU1} \equiv \left(\dot{\mathbf{q}}''_{\mathbf{o,s}}\right)_{\mathbf{1}} = \sigma(\mathbf{T_v^4 - T_\infty^4}) - \mathbf{h_f}(\mathbf{T_f - T_\infty}) + \dot{\mathbf{Q}}''_{\mathbf{o,s}}\left(\frac{\mathbf{L}}{\Delta \mathbf{h_c}}\right)$$

$$\approx \dot{\mathbf{q}}''_{\mathbf{o,ig}} - \dot{\mathbf{q}}''_{\mathbf{f}} + \dot{\mathbf{Q}}''_{\mathbf{o,s}}\left(\frac{\mathbf{L}}{\Delta \mathbf{h_c}}\right).$$

The critical energy flux $\dot{\mathbf{Q}}''_{\mathbf{o,s}}$ follows from flame length correlations and varies from about 50 to 100 kW/m^2. The combined heat flux from the material's (wall) flame and external heating must endure energy flux outputs in excess of $\dot{\mathbf{Q}}''_{\mathbf{o,s}}$ for spread to occur. Define, in keeping with Tewarson's parameters, *Critical Heat Release Rate, CHRR* ≡ $\dot{\mathbf{Q}}''_{\mathbf{o,s}}$ *~ 50 to 100 kW/m^2*:

CHFSU1 ~ CHF, HRP, CHRR, where **CHRR** is approximately constant. The burn-out criterion can apply if $\frac{\Delta \mathbf{h_c}}{\mathbf{L}}$ is large, perhaps greater than 4, and when

$$\frac{(\rho\delta)^{1/2}}{\left[\frac{\pi}{4}k\rho c\left(T_{ig}-T_{\infty}\right)^2\right]^{1/2}}$$

is small. Hence, the *burnout critical heat flux is approximately* (Eq. (102):

$$\left(\dot{q}''_{o,s}\right)_3 \equiv CHFSU3 \approx CHF\left(1-\frac{(\rho\delta)^{1/2}}{TRP}\right).$$

1.12 FLAMMABILITY DIAGRAMS

A graphical presentation of the processes of ignition, flame spread, burning and energy release rates is informative. The limits of these processes are just as important as their metric levels. We gave examples of data taken, and have illustrated some application to the vehicle material fire data. Indeed, Tewarson has made such plots in order to derive property parameters that are used in fire hazard assessment for materials. From the theoretical analyses presented here we have shown that such Flammability Diagrams are controlled by a limited set of material fire properties that underlie the Tewarson parameters. Let us summarize our results in terms of these Flammability Diagrams.

1.12.1 Burning and Energy Release Rate

Let us summarize our findings in Figure 4-22 for the burning and energy rates.

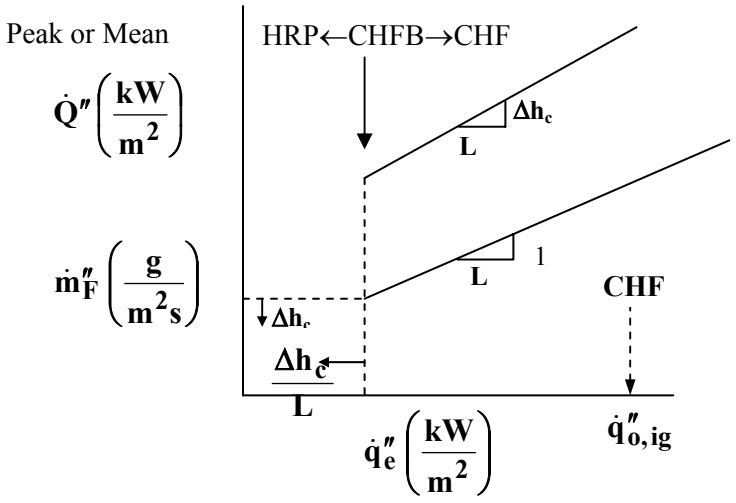

Figure 1-22 Burning rate characteristics.

The figure indicates that the **CHFB** increases with **CHF** and decreases with **HRP**. Hence, we conclude both the energy flux or **HRR** and its limits depend on **HRP**.

1.12.2 Ignition

Let us just consider thick materials, and the plot in Figure 1-23 illustrates ignition data trends.

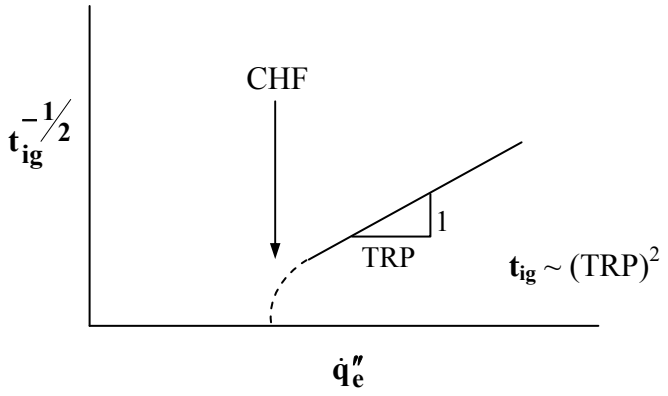

Figure 1-23 Ignition characteristics (thick materials)

The time to ignite depends on **TRP** and **CHF**.

1.12.3 Flame Spread – long heating time

Figure 1-24 summarizes the data trends for flame spread.

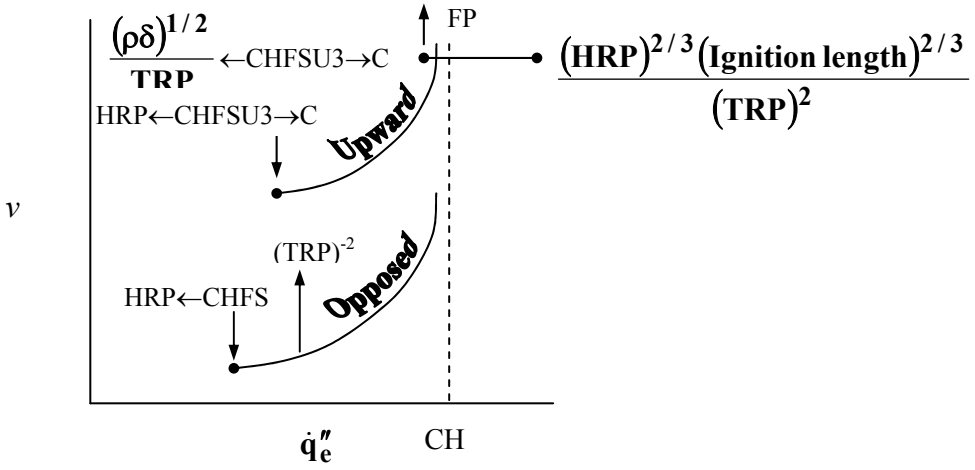

Figure 1-24 Flame spread characteristics.

The speed and limit fluxes dependencies are indicated.

1.12.4 Fire Hazard for Materials

For a specified heat exposure from the flame or other sources, the fire hazard potential of a material can be characterized by several measurable parameters introduced by Tewarson, which are related to approximate thermal, and combustion properties. Table 1-4 lists a summary of these parameters and their effects.

Table 1-4. Parameter Effects for Specified Heat Exposure of Materials

PARAMETER INCREASE	EFFECT
$\mathbf{HRP} \equiv \frac{\Delta h_c}{L}$ Heat release rate = **HRP** x $\dot{q}''_{net}$ (Eq. 40)	• Increases energy release rate. • Decreases critical heat flux for burning. • Increases upward flame speed. • Decrease critical heat flux for flame spread.
$\mathbf{TRP} \equiv \sqrt{\frac{\pi}{4}(k\rho c)}\left(T_{ig} - T_\infty\right)$ $t_{ig} = (\mathbf{TRP}/\dot{q}''_{net})^2$ (Eq. 20)	• Increases ignition time. • Decreases flame speed. • Increases critical flux for upward spread.
$\mathbf{CHF} \equiv \dot{q}''_{o,ig}$ (Eq. 18)	• Increases all other critical heat fluxes.
$\mathbf{FPI} \sim v^{1/2} \sim [(\mathbf{HRP}\ \mathrm{x}\ \dot{q}''_{net})^{1/3}/\mathbf{TRP}]$ (Section 1.11.2)	• Increased flame speed
Thickness	• Decreases critical flux for upward spread.
Ignition Length	• Increases upward flame speed.

The thickness of the material governs the thermally thick or thin behavior and the ignition length may explain the behavior of tests using small ignition sources.

*The conclusion from this analysis is that the measurable parameters HRP, CHF, and TRP in combination with the heat flux from the flame and other sources are the primary material properties controlling flammability. Ignition length is important for upward flame spread***.** The three property parameters can explain most of the behavior of the fire processes with external heat flux including their lower limit critical values. While the process behavior has been substantiated in experimental data, the limit conditions lack sufficient data to test these results. Yet the analyses are reasonably complete to give full confidence to the theoretical findings. These results have profound implications for flammability testing, and could put the multitude of diverse test methods on a sound scientific and universal track. Of course, the heat of gasification is a property hiding decomposition chemistry and transient effects, and that will

require its decomposition into more fundamental properties to make it more understandable. However, it is measurable, and limitations in using a global heat of gasification can suffice for now.

NOMENCLATURE

a	Parameter, Eq. (80)
A	Pre-exponential factor
c_p	Specific heat at constant pressure
k	Thermal conductivity
h_c	Convective heat transfer coefficient
h_r	Radiative heat transfer coefficient
h_t	Total heat transfer coefficient
Δh_c	Heat of combustion
h_{fg}	Heat of vaporization
L	Heat of gasification
$\dot{m}''_F$	Mass loss rate of fuel per unit area (flux)
$\dot{m}''_o$	Critical mass flux of water
$\dot{q}''_{f,c}$	Convective heat flux from the flame
$\dot{q}''_e$	External radiant heat flux
$\dot{q}''_{f.r}$	Radiant heat flux from flame
T_f	Flame temperature
T_o	Initial temperature
T_s	Temperature of the surface of the fuel
T_v	Vaporization temperature of the fuel
T_∞	Ambient temperature
v	Velocity
$Y_{F,o}$	Fuel mass fraction in the condensed phase
$Y_{ox,\infty}$	Oxygen mass fraction the ambient

$\mathbf{X_r}$	Flame radiation fraction
β	Parameter, Eq. (53)
δ	Thickness
ρ	Density
σ	Stefan-Boltzmann constant

Subscripts

b	Burning
c	Convective
crit	Critical
f	Flame
ig	Ignition
o	Initial, critical limit
p	Pyrolysis
r	Radiative
s	Spread, surface
t	Total
v	Vaporization

REFERENCES

1. Test Method for Determining Material Ignition and Flame Spread Properties, ASTM E 1321, ASTM International, Conshohacken, PA.

2. Test Methods for Measurement of Synthetic Polymer Material Flammability Using a Fire Propagation Apparatus (FPA), ASTM E 2058, ASTM International, Conshohacken, PA.

3. Test Method for Heat and Visible Smoke Release Rates for Materials and Products Using an Oxygen Consumption Calorimeter, ASTM E 1354, ASTM International, Conshohacken, PA.

4. Panagioutou, J. and Quintiere, J. G., "Generalizing Flammability of Materials", Interflam 2004, Edinburgh, July 2004.

5. Test Method for Critical Radiant Flux of floor-Covering Systems Using a Radiant Heat Energy Source, ASTM E 648, ASTM International, Conshohacken, PA.

6. Test Method for Determination of Fire and Thermal Parameters of Materials, Products, and Systems Using an Intermediate Scale Calorimeter (ICAL), ASTM E 1623, ASTM International, Conshohacken, PA.

7. Quintiere, J. G. and Rangwala, A. S., "A Theory for Flame Extinction based on Flame Temperature", *Fire and Materials*, Vol. 28, 387-402, 2004.

8. Siegel, R. and Howell, J. R. *Thermal Radiation Heat Transfer, 2nd. Ed.*, McGraw-Hill Book Co., New York, 1981, p. 618.

9. Flammability of Interior Materials, FMVSS 302, U. S. Dept. of Transportation, Nat. Highway and Safety Admin., Washington, DC.

10. de Ris, J. "The Spread of a Laminar Diffusion Flame", 12th Symposium. Int. on Combustion, the Combustion Institute, Pittsburgh, PA, 1969, pp. 241-252.

11. Quintiere, J. G., "The Effect of Angular Orientation on Flame Spread over Thin Materials", *Fire Safety Journal*, **36**, (3), 291-312, 2001.

CHAPTER II

TOXICITY TEST METHODS

D.A. Purser, Fire Safety Engineering Centre BRE, Garston, Watford, UK

2.1 INTRODUCTION

The toxic hazard to an occupant of a passenger compartment during a vehicle fire depends upon [1]:

1. The time-concentration curves for the major toxic products at the breathing zone of the occupants, which in turn depend upon:
   a) The fire growth curve in terms of the mass loss rate of the fuel ($kg.s^{-1}$) and the volume into which it is dispersed (m^3) to provide a mass loss concentration term ($kg.m^{-3}$) changing with time throughout the fire;
   b) The yield of toxic products, smoke, and heat in the fire (for example kg CO per kg of material burned).
2. The toxic potency of the effluent (the exposure concentration [$kg.m^{-3}$], or exposure dose [$kg.m^{-3}$.min or ppm.min] required to cause toxic effects. This term requires consideration of three aspects:
   a) Exposure concentrations or doses likely to impair or reduce the efficiency of escape due to psychological and/or physiological effects;
   b) Exposure concentrations or doses likely to produce incapacitation or prevent egress due to psychological and/or physiological effects;
   c) Lethal exposure concentrations or doses.

The time-concentration curves for toxic products can be measured directly in large-scale tests as reported in the Volume I. The toxic effects and toxic potencies can be predicted from the toxicity data on individual fire gases obtained from human or animal experimentation. The two terms can be combined in toxic hazard assessment models such as the Purser SFPE model [1], the FAA combined Hazard Survival Model [2] or the ISO TS 13571 toxic hazard model [3]. All of these are reasonably similar in their approaches and results, as discussed in Volume I. They can be used to predict time and exposure dose to incapacitation and death.

Another approach is to obtain data on the performance of individual products or materials from small-scale tests and use the data as input to fire hazard modelling. The most important parameters are the mass burning rate (kg/s) (or heat release rate from which the mass burning rate can be calculated) and the yields of key toxic products (g/g) (see Volume III).

2.2 VARIABLES AFFECTING TOXIC PRODUCT YIELDS AND REQUIREMENTS FOR TOXICITY TESTS

The toxic potency of effluents depends upon the yield of key toxic products. Toxic product yield in fires depends upon three main variables:

- The elemental composition of the material
- The organic composition of the material
- The combustion conditions

Of these, the most important are the elemental composition and the combustion conditions. The elemental composition limits the range of major toxic gases that can be formed and influences their yields. For example, hydrogen chloride can be evolved only if chlorine is present in the material, but chlorine is also a fire retardant element, which reduces the efficiency of combustion of carbon in a material and thereby increases CO yield.

The combustion conditions are extremely important determinants of product yields. Non-flaming pyrolysis in air produces high yields of CO, other toxic gases and smoke, but low yields of CO_2. For flaming combustion the product yields are highly dependent upon the fuel/air ratio, as discussed in Volumes I and III. Lower fuel/air ratios (equivalence ratios < 1) result in well-ventilated flaming conditions, with low yields of CO and other toxic gases. Higher fuel/air ratios (equivalence ratios > 1) produce high yields of CO and other toxic gases. For example, the yield of CO from burning polymethylmethacrylate (PMMA) varies by a factor of 50 or so between well ventilated and vitiated (fuel rich) combustion conditions (see Figure 2-1). It is, therefore, important that it is possible for the combustion conditions in any small-scale toxicity test to be defined in terms of fuel/air ratio and flaming/non-flaming conditions, so that the combustion conditions in the test (and the yields of toxic products obtained) can be related to those in the full-scale vehicle fire scenarios.

2.3 TREATMENT OF TEST DATA AND SURVIVAL MODEL

The most effective method for making use of the data obtained from various tests would be to set a performance standard for a vehicle in terms of predicted occupant survival time. The endpoint chosen would depend upon the objective. If the objective is survival following rescue then time to incapacitation could be a suitable endpoint. If the objective is the ability to escape then a somewhat more conservative endpoint may be indicated. ISO TC/92 SC3 has proposed use of 0.3 x the FED for incapacitation as a possible design limit for building fires [24].

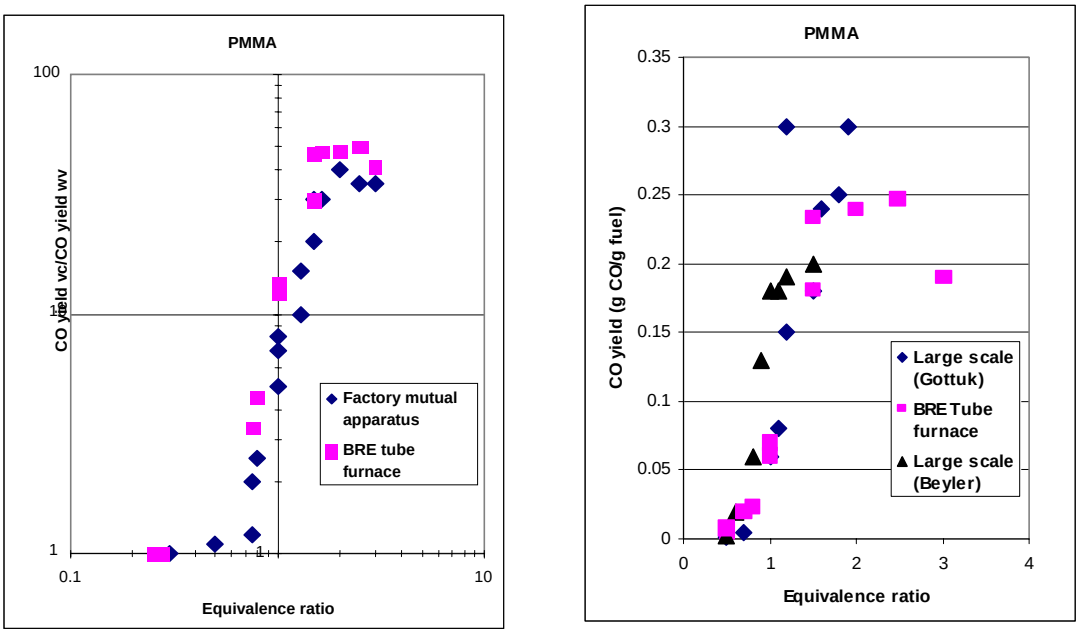

Figure 2-1: Comparison of CO yield ratio* (left figure) and CO yield (right figure) as a function of equivalence ratio for PMMA in the BRE tube furnace, compared with ASTM E 2058 Fire Propagation Apparatus and large-scale compartment fires. (* CO yield ratio is the ratio of the CO yield obtained at any equivalence ratio divided by that obtained under well-ventilated conditions) (From Purser [4]).

Having selected an endpoint condition, the test data could be used to calculate time to this predicted endpoint for a fire involving the test material or product. The decomposition rate data would be used to measure the mass loss rate per unit area of the specimen under non-flaming conditions, the time to ignition, and the mass loss rate per unit area (fire growth curve) under vitiated flaming combustion conditions. The mass loss rate data would be multiplied by the yield

data to provide the rates of evolution of key toxic gases (e.g. CO g/s). From the mass loss rates, the concentration-time curves for the gas are then calculated for a given enclosure volume (for example the volume of an enclosed vehicle passenger compartment). FED calculations are then used to calculate predicted time to FED 0.3. Different materials could then be ranked according to their time to FED 0.3 and selected based on a performance criterion.

The method could be validated against a full-scale test reference scenario. In order to achieve this result from the small-scale tests and predicted FED times would need to be compared with those obtained in full-scale vehicle fire tests. Once the validity of a suitable test and calculation protocol has been established, this could be adopted as a requirement. The full-scale test reference scenario could then be used if a regulator or vehicle manufacturer was unwilling to accept the results of the small-scale tests and calculation protocol. The full-scale reference scenario (or scenarios) would need to have a specified standard initial fire(s) as an ignition source(s) in either a crashed or un-crashed vehicle with specified cabin ventilation conditions (side windows up or down). One approach might be to use the small-scale tests protocol for in-house development purposes or for minor model modifications, and the full-scale test reference scenario in order to qualify a new vehicle design.

2.4 FIVE TOXICITY TEST METHODS FOR APPLICATION TO AUTOMOTIVE MATERIALS

The following test methods are cited for consideration in relation to toxicity testing of vehicle polymers and polymer parts:

1. ASTM E 2058 Fire Propagation Apparatus [5];
2. ASTM E 1354 Cone Calorimeter [6];
3. ASTM E 662 NBS Smoke Chamber and IMO Smoke Toxicity Test Procedure (SwRI) [7];
4. Airbus Industries ABD 0031 [8];
5. IEC 60695-7-50 Tube Furnace Method [9].

The E 2058 Fire Propagation Apparatus [5] has been used to provide a database of product toxic product yields for a wide range of materials under a wide range of defined combustion conditions (Volume III). The data can be expressed as yields (g/g) and the combustion conditions can be related to those in intermediate and large-scale tests (and have been for this project). The data can be directly applied to modeling toxic hazards in vehicle fires. *The method*

also has the advantage that both heat release rate and toxic product yields can be measured in the same test.

The E 1354 Cone Calorimeter [6] has also been used to measure toxic products yields**.** *It also has the advantage that both heat release rate and toxic product yields can be measured in the same test.* The apparatus was primarily designed for the measurement of heat release rate. *It has serious disadvantages with respect to measurement of toxic product yields* in that:

- It replicates only non-flaming or well ventilated combustion conditions;
- The high level of dilution in the hood results in high thresholds of detection and quantification for toxic products (so that only products evolved at high concentrations can be measured);
- Evolved gases have a significant contact time with metal surfaces in the ductwork, which may result in losses of toxic acid gases (low recoveries of acid gases, such as HCl).

The E 662 NBS Smoke Chamber with the Airbus or IMO and ABD 0031 Test Procedures [7,8] enables measurement of concentrations of toxic gases at defined times during which a sample of material is exposed to radiant heating in an enclosed metal and glass chamber. The apparatus was originally designed for smoke measurement. It has a number of serious disadvantages with respect to measurement of toxic product yields in that:

- It consists of a primitive fire model (radiant heating of a specimen in a small closed chamber with no control or measurement of combustion conditions that cannot be readily related to actual fire conditions);
- Toxicity results are expressed in the form of a simplistic index with a poor basis in terms of relationship to toxic hazards;
- The static chamber design results in considerable losses of important toxic products such as acid gases to the chamber walls, producing low recoveries of acid gases from materials;
- *It is considered that the results obtained have limited value or relevance to toxic fire hazards***;**

Despite these shortcomings, the method has the advantage that it is used for specification purposes with respect to toxicity in IMO and in the European Aircraft and Railway industries.

Another recently developed small-scale test method that enables toxic product yields to be measured over a wide range of combustion conditions is the ISO/IEC 60695-7-50 tube furnace method [9]. This could be considered as an alternative to the E 2058 method. This method has the following advantages:

- It enables replication of a wide range of combustion conditions including non-flaming decomposition and vitiated combustion conditions;
- The products are measured on a "flow through" basis with short residence times and minimal metal surfaces. This minimizes losses to apparatus walls and provides high recoveries of acid gases;
- Product yields are calculated based upon sample mass loss;
- The method is published as an ISO/IEC Technical specification and a British Standard.

A disadvantage of the method is that it does not enable measurements of fire growth rate.

2.5 SWRI STUDY ON THE COMPARISON OF FIRE PROPERTIES OF AUTOMOTIVE MATERIALS AND EVALUATION OF PERFORMANCE LEVELS

The SwRI report [10] contains the results of small-scale and intermediate-scale tests on 18 exterior automotive parts (i.e. parts not in the passenger compartment). Small-scale tests were conducted using the Cone Calorimeter (ASTM E 1354) to obtain data on ignition, heat release, smoke and toxic gas production data using a range of heat fluxes to obtain non-flaming and well-ventilated flaming decomposition conditions. In addition, toxic product yield data were obtained using the ASTM E 662 Smoke Chamber in combination with two different combustion methods. One method was the Airbus Industries ABD 0031 method, which uses a conical furnace to irradiate a vertical specimen. The other method was the IMO Smoke Toxicity Test Procedure, which uses a horizontally-mounted specimen irradiated using a conical furnace. Gases from all three methods were analyzed using FTIR. The authors also discuss the toxicity index procedures used to rank specimen performance in the Airbus and IMO methods.

An important aspect of any toxic hazard assessment method is prediction of the fire growth curve (heat release rate or fuel mass loss rate curve). The authors develop an interesting procedure for estimating predicted full-scale fire growth for the materials tested based upon the

time to ignition and peak heat release rate in the Cone Calorimeter. This may be applied usefully to hazard assessments and materials specification for vehicle passenger compartment and vehicle exterior materials.

The other most important aspect of a toxic hazard is to obtain toxic product yield data for materials under the conditions occurring in vehicle fires. The materials tested in this study excluded the passenger compartment materials, as they were measured in the previous GM sponsored study at SwRI . As discussed in a previous section, based upon the results of the large-scale vehicle fire study, it is considered that measurements of toxic product yield could be most useful for passenger compartment materials. Toxic product yields from engine and other external fires were found to have little or no significance for vehicle occupant survival. However, it is useful to examine the performance of the tests used for the SwRI study, since they could equally well be applied to passenger compartment materials.

The important considerations are the extent to which the test methods replicate the decomposition conditions and toxic product yields in the large-scale fire tests. This can be done by an examination of the CO/CO_2 ratios and CO yields obtained, compared with those in the large-scale vehicle fire tests. It is also important to examine the extent to which the test methods are capable of providing accurate measurements of key toxic gases evolved, in particular acid gases such as HCl, in addition to CO and CO_2. This can be achieved by an examination of the recovery of elemental chorine as HCl in the tests. PVC is a useful material in this context, since almost 100% dehydrochlorination occurs when PVC is heated above 300°C or when it burns in flaming mode [11,12]. PVC contains 57.3% chlorine, so the HCl yield in a small-scale test should approach 573 mg/g (depending upon the PVC formulation).

2.5.1 Toxic Product Yield Data from the SwRI Small-Scale Tests

The main small-scale method used for the 18 materials was the Cone Calorimeter. Tests were conducted at heat fluxes of 20, 35 and 50 kW/m^2. The results for flaming decomposition at 50 kW/m^2 were used to calculate yields of CO, HCN and HCl as appropriate, depending upon the composition of the material tested. Three materials were chosen for the Airbus and IMO tests, including materials producing low, medium and high CO yields in the Cone tests (Volumes I and III):

1. Headlight lens – Clean Lens (4857041A) - polycarbonate

2. Hoodliner Face (4716832) PET

3. Kick Panel Insulation Backing – Rubber side (4860446) PVC

An initial comparison has been made for CO yields obtained from the Cone Calorimeter for 5 materials with data obtained under well-ventilated combustion conditions measured in the ASTM E 2058 Fire Propagation Apparatus [Volume III]. These data together with additional data from a variant of the IEC tube furnace method (BS7990 tube furnace protocol) [9] have been compared.

The data from the E2058 FPA apparatus and the Cone Calorimeter are in good agreement except for nylon and PVC. The important point however, is that these data were both obtained using well-ventilated flaming combustion conditions. In actual fires (as shown in Figure 2-1), the yield of CO from non-fire retarded materials varies significantly with the combustion conditions. Both the E 2058 and the IEC tube furnace methods are capable of addressing a range of combustion conditions, which can be designated in terms of Φ (the fuel/air equivalence ratio), such as in Figure 2-1. In the figure, there is a good agreement between CO yields obtained by the E 2058 and IEC tube furnace expressed in terms of Φ.

Figure 2-2 illustrates the wide range of CO yields obtained in the passenger compartments during the large-scale vehicle fire tests compared with the range of CO yields obtained for 18 automotive exterior materials using the Cone Calorimeter and that obtained for a range of common polymers under a range of combustion conditions using the IEC tube furnace method. As the figure shows, the Cone results are clustered in the low CO yield range (representing well-ventilated combustion) for the majority of materials. Only one material (PET) gave a fairly high CO yield in the Cone Calorimeter. This contrasts with the large-scale vehicle fire test data, which covers a wide range from 25-50 to 600-625 mg CO/g fuel. The data from the IEC tube furnace cover almost the same range as the large-scale fire tests, from 0-25 mg/g up to 525-550 mg CO/g fuel, the actual yield depending upon the equivalence ratio set.

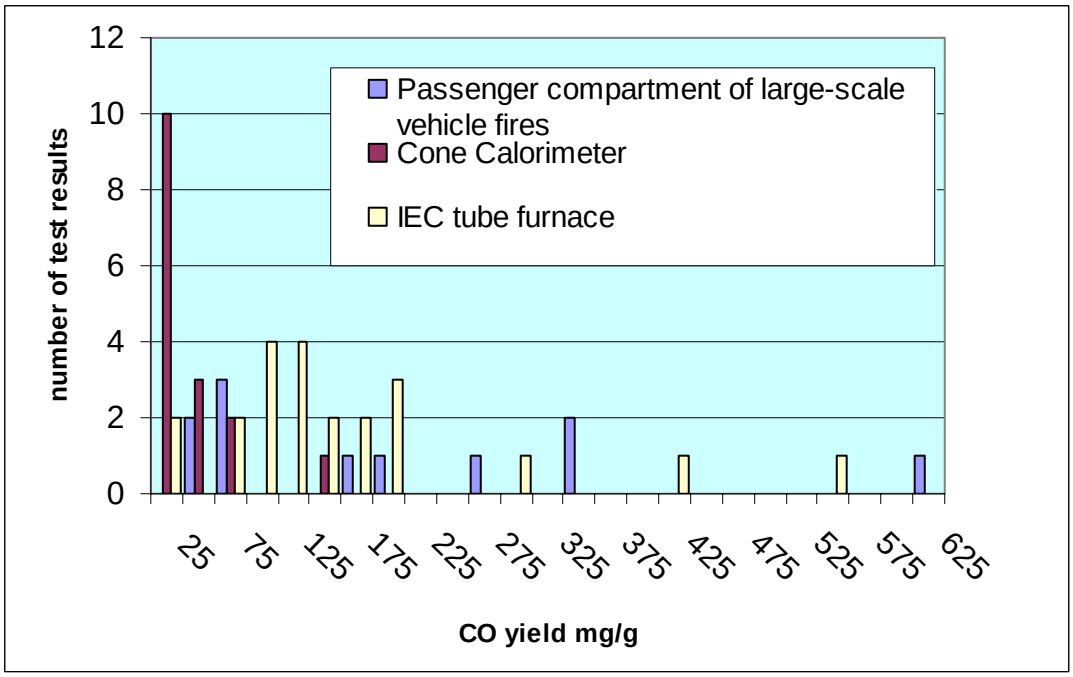

Figure 2-2: Comparison of range of CO yields obtained in large-scale vehicle fire tests, the 18 automotive materials in the Cone Calorimeter and data from a range of common polymers under a range of combustion conditions in the IEC tube furnace.

For the PVC material in the SwRI tests, the HCl yield was measured at 2.7 mg/g. Assuming the material was 100% PVC this represents an exceptionally low recovery of 0.5% of HCl likely to have been evolved from the specimen. This compares with recovery figures from the IEC furnace of 516 mg/g representing 88% recovery of chlorine in the material [11, 12]. It is of course possible that the Kick Panel material was plasticized PVC, which typically contains approximately 50% PVC polymer. This would reduce the anticipated HCl yield to approximately 200 mg/g. The low HCl recovery could also be due to loss of HCl on the Cone heater and instrumentation problems.

Data are also presented in the SwRI report for CO and HCl yields for the three materials using the two versions of the smoke box test. It is not clear how this is achieved for the Airbus test since there is no load cell to measure mass loss. Details of how yields were calculated are not supplied in the report. The results are shown in Table 2-1 for the three materials under flaming conditions.

Table 2.1.Yields (mg/g) of CO and HCl Obtained from Three Automotive Materials Using Three Toxicity Test Methods

Part	Cone calorimeter	Airbus	IMO
Headlight (PC)	50	25.8	1.1
Hoodliner (PET)	142	82.2	90.2
Kick Panel (PVC)	9.0	29.5	6.4
HCl yield (PVC)	2.7	27 (non-flaming)	

The CO yields are generally low except for the PET, and very low for two materials using the IMO test protocol. The HCl yield in the Airbus test is an order of magnitude higher than that obtained using the Cone Calorimeter but still another order of magnitude less than would be predicted from the chlorine content of PVC and the results obtained using the IEC method**.** It is suggested that none of these three methods (Cone calorimeter, Airbus or IMO) provide an adequate test for measuring toxic product yields from materials to be used in vehicles**.**

2.6 BEST SMALL-SCALE TEST METHODS FOR THE TOXICITY ASSESSMENT OF AUTOMOTIVE PRODUCTS

The review of five test methods for consideration in relation to toxicity testing of vehicle polymers and polymer parts suggest that tests using ASTM E2058 FPA and ISO/IEC 60695-7-60 provide data directly applicable to the assessment of toxic hazards in vehicle fires. Thus, either method could be selected as a standard test method for toxicity.

REFERENCES

1. Purser, D.A., "Toxicity Assessment of Combustion Products", *The SFPE Handbook of Fire Protection Engineering (3rd ed)*, DiNenno P.J., (ed.), National Fire Protection Association, Quincy, MA 02269, 2002, pp. 2/83 – 2/171.

2. Speitel, L.C., Toxicity Assessment of Combined Gases and Development of a Survival Model. DOT/FAA/AR-95-5. July 1995.

3. Life threat from fires — Guidance on the estimation of time available for escape using fire data ISO/IEC TS 13571 2001.

4. Purser, D.A., ASET and RSET: Addressing Some Issues in Relation to Occupant Behavior and Tenability. 7th International Symposium on Fire Safety Science. Worcester Polytechnic Institute – Worcester, Massachusetts, USA. 16-21 June 2002. Proceedings.

5. ASTM E 2058 Fire Propagation Apparatus (FM Global Research).

6. ASTM E 1354 Cone Calorimeter

7. ASTM E 662 NBS Smoke Chamber with IMO FTP Toxicity Code.

8. ASTM E 662 NBS Smoke Chamber with Airbus Industries ABD 0031 Toxicity Protocol.

9. ISO/IEC TS 60695-7-60 Tube Furnace Toxicity Test Apparatus and Variant Protocol: Tube Furnace Method for the Determination of Toxic Product Yields in Fire Effluents BS7990 2003.

10. Battipaglia, K.C., Griffith, A.L., Huczek, J.P., Janssens, M.L., Miller, M.A., and Wilson, K.R., Comparison of Fire Properties of Automotive Materials and Evaluation of Performance Levels. Draft Final Report SwRI Project No 01.05804, September 2003.

11. Purser, D.A. and Purser, J.A., The Potential for Including Fire Chemistry and Toxicity in Fire Safety Engineering. BRE Project Report 202804, 26th March 2003.

12. Purser, D.A., Fardell, P., Rowley, J., Vollam, S., Bridgeman, B. and Ness, E.M.,"An improved tube furnace method for the generation and measurement of toxic combustion products under a wide range of fire conditions", Flame Retardants Conference - Proceedings, Interscience Communications, London. UK, pp 263-274, 1994.

CHAPTER III
TEST METHODS FOR THE FIRE BEHAVIOR OF MATERIALS FOR THE TRANSPORTATION INDUSTRY

A. Tewarson, FM Global. Norwood, MA, USA

3.1. DOT TESTING METHODS FOR MATERIALS IN VEHICLES

For materials used in the transportation vehicles, following test methods are specified in the DOT regulation, which are summarized in Table 3-1:

1. National Highway Traffic Safety Administration: NHTSA-DOT Standard 302 test for materials used in the automobile passenger compartment [1];
2. Federal Aviation Administration: FAA-DOT required fire tests for aircraft materials [2];
3. Federal Railroad Administration: FRA required fire tests for materials used in passenger cars and locomotive cabs [3];
4. Federal Transit Administration: FTA recommendations for testing of transit bus and van materials [4];
5. U.S. Coast Guard: USCG fire test standards for passenger vessels [5]. In general larger-scale tests are used (IMO fire test procedures).

Table 3-1. Test Methods Specified in the DOT Regulations

Agency	Test Standard	Application
NHTSA-DOT [1]	FMVSS 302	Materials used in passenger cars, multipurpose vehicles, trucks, and buses.
FRA [3], **FTA** [4]	ASTM D3675-98	**FRA** (passenger rail cars and locomotive cabs): cushions, mattresses: $I_s \leq 25$; vehicle components (flexible cellular foams): $I_s \leq 25$. **FTA** (bus and van materials): seating cushion: $I_s \leq 25$
FRA[3], **FTA** [4]	ASTM 162-98	**FRA** (passenger rail cars and locomotive cabs): all vehicle components*: $I_s \leq 35$; vehicle light transmitting plastics: $I_s \leq 100$. **FTA** (bus and van materials): seating frame, seating shroud, panel walls, ceiling, partition, windscreen, HVAC ducting, and light diffuser, exterior shells: $I_s \leq 35$; insulation thermal and acoustic: $I_s \leq 25$
FAA [2]	FAR 25.853 (horizontal test)	Aircraft cabin, cargo compartment, and miscellaneous materials: burn rate ≤ 2.5 in/min or ≤ 4 in/min
FAA [2]	FAR 25.853 (heat release test, 35 kW/m^2 heat exposure)	Aircraft cabin materials: average maximum heat release rate ≤ 65 kW/m^2 (5-minute test) and ≤ 65 kW-min/m^2 or 3.9 MJ/m^2 (first two minutes).

Table 3-1 continued on the next page

Table 3-1 continuing from the previous page

Agency	Test Standard	Application
FRA [3]	ANSI/IEEE383-1974	Passenger rail cars and locomotive cabs: power cable
FRA [3], **FTA** [4], **FAA** [2]	ASTM E 662-97 (also FAR 25.853: smoke generating characteristics at 25 kW/m^2 heat exposure used by FAA)	**FRA** (passenger rail cars and locomotive cabs): cushions, mattresses: D_s (1.5) ≤ 100; D_s (4.0) ≤ 175; fabrics: D_s (4.0) ≤ 200; all vehicle components*: D_s (1.5) ≤ 100; D_s (4.0) ≤ 200; vehicle components (flexible cellular foams): D_s (1.5) ≤ 100; D_s (4.0) ≤ 175; vehicle floor covering: D_s (1.5) ≤ 100; D_s (4.0) ≤ 200; vehicle light transmitting plastics: D_s (1.5) ≤ 100; D_s (4.0) ≤ 200; vehicle components (elastomers): D_s (1.5) ≤ 100; D_s (4.0) ≤ 200; low voltage wire and cable and power cable: D_s (4.0) ≤ 200 (flaming); D_s (4.0) ≤ 75 (non-flaming). **FTA** (bus and van materials): seating cushion, frame, and shroud, panel walls, ceiling, partition, windscreen, and HVAC ducting, exterior shells: D_s (1.5) ≤ 100; D_s (4.0) ≤ 200; seating upholstery: D_s (4.0) ≤ 250 (coated); D_s (4.0) ≤ 100 (uncoated); panel light diffuser, insulation thermal and acoustic: D_s (4.0) ≤ 100. **FAA** (Aircraft): cabin materials: D_m (4.0 min) ≤ 200
FRA [3], **FTA** [4], **FAA** [2]	FAR 25.855 (vertical test)	**FRA** (passenger rail cars and locomotive cabs): fabrics: flame time ≤ 10 seconds; burn length ≤ 6 in. **FTA** (bus and van materials): seating upholstery: flame time ≤ 10 seconds; burn length ≤ 6 in. **FAA** (Aircraft): cabin and cargo compartment materials: flame time ≤ 15 seconds; burn length ≤ 6-in
FRA [3], **FTA** [4]	ASTM E648-97	**FRA** (passenger rail cars and locomotive cabs): vehicle floor covering: C.R.F ≥ 5 kW/m^2 **FTA** (bus and van materials): flooring covering: C.R.F ≥ 5 kW/m^2
FRA [3]	ASTM C 1166-91	Passenger rail cars and locomotive cabs: vehicle components (elastomers): pass
FRA [3]	NEMA WC 3/ICEA S-19-1981/UL 44 and UL 83	Passenger cars and locomotive cabs: low voltage wire and cable: pass
FRA [3], **FTA** [4]	ASTM E119-98	**FRA** (passenger rail cars and locomotive cabs): pass. **FTA** (bus and van materials): flooring wheel well and structure and fire wall: pass

FAR: Federal Aviation Regulations

Some of the popular small-scale test methods, listed in Table 3-1, are presented in the following sections.

3-1-1. The FMVSS 302 Test for the Flammability of Vehicle Interior Materials

The standard specifies burn resistance requirements for materials used in the occupant compartments of motor vehicles [1]. The purpose of the standard is to reduce the deaths and injuries to motor vehicle occupants caused by vehicle fires, especially those originating in the interior of the vehicles from sources such as matches or cigarettes. The standard applies to passenger cars, multipurpose passenger vehicles, trucks, and buses.

Acceptance Criteria

The materials shall not burn nor transmit a flame front across its surface at a rate of more than 102 mm/min (1.7 mm/s). If a material stops burning after 60 seconds of heat exposure and has not burned more than 51-mm from the point where the timing was started, it shall be considered to meet the burn-rate requirement.

Test Conditions

The test is performed in a 381-mm long, 203-mm deep and 356-mm high metal cabinet, shown in Fig. 3-1. It has a glass observation window in the front, an opening to permit insertion of the specimen holder and a hole to accommodate tubing for gas burner. For ventilation, it has a 13-mm clearance space around the top of the cabinet, ten hole in the base of the cabinet, each hole 19-mm in diameter and legs to elevate the bottom of the cabinet by 10-mm.

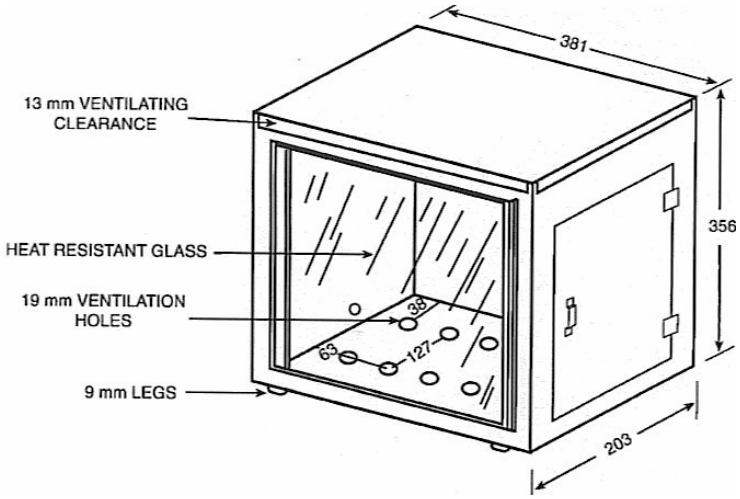

Figure 3-1. The FMVSS 571.302 standard test chamber. Figure taken from Ref. 1.

The test specimen is inserted between the two U-shaped frames of metal stock, 25-mm wide and 10-mm high. The interior dimensions of the U-shaped frame are 51-mm wide by 330-mm long. The total width of the frame is 101-mm. A specimen that softens and bends is kept horizontal by supports consisting of 10-mil heat - resistant wires at 25-mm intervals, inserted over the bottom U-shaped frame. The U-shaped frames hold both sides and one end of the sample even with the open end of the frame.

The ignition source consists of a Bunsen burner with a tube of 10-mm inside diameter. Gas supply is adjusted to provide a vertical, 38-mm high flame. The air inlet to the burner is closed. The gas used in the burner has a flame temperature equivalent to that of natural gas.

Each specimen is rectangular, 102-mm in width and 356-mm in length. The thickness of the specimen is that of the single or composite material used in the vehicle, except that if the thickness exceeds 13-mm, it is cut down to that thickness measured from the surface of the specimen closest to the occupant compartment air space. If the specimens are not flat, they are cut to not more than 13-mm in thickness at any point. The maximum available length or width of a specimen is used where either dimension is less than 356-mm or 102-mm respectively, unless surrogate testing is required. Prior to testing, each specimen is condition for 24 hours at a temperature of 21 ^{o}C and a relative humidity of 50%. The test is conducted under ambient conditions.

The Bunsen burner is placed under the horizontal sample such that the center of the burner tip is 19-mm below the center of the bottom edge of the open end of the sample. The sample is exposed to the flame for 15 seconds. The time for the flame to reach 38-mm from the open end of the sample is noted and used to calculate the burn rate in mm/min.

3-1-2. ASTM D3675-98: Standard Test Method for the Surface Flammability of Flexible Cellular Materials using a Radiant Energy Source

The test standard covers testing the flammability and smoke emission characteristics of materials used in the construction of vehicles [3,4].

Radiant Panel: The panel is 300- x 460-mm (12- x 18-in) in area with a vertical orientation. The maximum radiant panel output at the top of the specimen is equivalent to a black body temperature of 670 ± 4 ^{0}C (45 kW/m^{2}).

Specimen Dimensions and wrapping: The specimen is 150- x 460-mm (6-x 18-in) in area, inclined in front of the radiant panel. Specimens with thickness < 25-mm are tested at their maximum thicknesses produced. Back and sides of the specimens are wrapped with 0.05-mm (0.002-in) thick aluminum foil with shiny side against the specimen. 6.4-mm (0.25-in) thick insulation board is used as the backing. The specimen is held in the holder by a 150-mm x 460-

mm (6- x 18-in) sheet of 25-mm (1-in) 20 gage hexagonal steel wire mesh placed against the exposed face of the specimen.

Specimen Orientation: The specimen is oriented vertically at an angle to the vertical radiant panel such that the top of the specimen is closer to the radiant panel, forcing the ignition near its upper edge and the flame front to progress in the downward direction.

Measurements: Measurements are made for: 1) time of the arrival of the flame at each of the 75-mm (3-in) marks on the specimen holder and 2) maximum temperature rise of the stack thermocouples.

Test Duration: Each test is completed when the flame reaches the full length of the specimen or after an exposure time of 15-minutes, whichever occurs earlier, provided the maximum temperature of the stack thermocouples is reached.

Calculation: Flame spread index ($\mathbf{I_s}$) is calculated from the measured data, defined as the product of flame spread factor, $\mathbf{F_s}$, and the heat evolution factor, **Q**.

Fire Behavior Being Examined: This is fire-test response standard. In the test downward flame spread rate and associated heat release rate in the presence of decreasing external heat exposure are examined.

Agencies Using the Test: The following agencies use this test: 1) FRA: for cushions and mattresses and flexible cellular foams used as vehicle components and 2) FTA for seating cushions for bus and vans.

3-1-3. ASTM E162-98: Standard Test Method for the Surface Flammability of Materials Using a Radiant Energy Source

This test methodology is the same as ASTM D 3675-98, however, it is to be used for research and development purposes [3,4]. It is not intended for use as a basis of ratings for building code purposes. Specimens are prepared differently for materials applied as substrates, opaque sheet materials, liquid films, and fabrics.

3-1-4. ASTM E662-97: Standard Test Method for the Specific Optical Density of Smoke Generated by Solid Materials

This fire-test-response standard determines the specific optical density of smoke generated by solid materials and assemblies mounted in the vertical position in thicknesses up to and including 1-in (25-mm) [2,3,4].

Radiant Heat Furnace: An electric furnace with a 3-in (76-mm) diameter opening providing a constant irradiance of 25 kW/m^2 on the specimen surface is used. The furnace is placed in a test chamber with inside dimensions of width x depth x height of 36- x 24- x 36-in (914- x 610-x 914-mm). The test is performed in the closed chamber.

Specimen Dimensions and wrapping: Specimens with dimensions of 3- x 3-in (76- x 76-mm) with thickness up to and including 1-in (25-mm) are used. The specimen orientation has no significant effect on the test results. A holder holds the specimen in place. All the samples are covered across the back, along the edges, and over the front surface periphery with a single 0.04-mm thick aluminum sheet with dull side in contact with the specimen. The specimens are backed with a 0.5-in (13-mm) thick sheet of inorganic insulation millboard. A pilot flame burner is used for flaming test, whereas the burner is not used for non-flaming tests.

Measurements: Measurements are made for: 1) light transmittance and corresponding time either as a continuous plot with a multi range recorder or a time intervals no greater than 30 second with a multi range meter readout.

Test Duration: Test is continued for 3-minutes after a minimum light transmittance value is reached or for 20 minutes, whichever occurs first.

Calculation: The specific optical density, $\mathbf{D_s}$, is calculated at any time as follows:

$$\mathbf{D_s = (V/AL)\log_{10}(100/T)} \quad (1)$$

where **V** is the volume of the closed chamber (ft^3 or m^3), **A** is the exposed area of the specimen, (ft^2 or m^2), **L** is the optical path length through the smoke (ft or m), and **T** is the percent light transmittance as read from the light sensing instrument.

Fire Behavior Being Examined: Light obscuration property of smoke in flaming and non-flaming fires is used to examine the fire behavior of materials in terms of smoke release.

Agencies Using the Test: The following agencies use this test: 1) FRA: for cushions, mattresses and flexible cellular foams used as vehicle components, 2) FTA for seating cushions for bus and vans, and 3) FAA for aircraft cabin materials.

3-1-5. FAR 25.853 AND FAR 25.855: Bunsen Burner Test for the Vertical Aircraft Cabin and Cargo Compartment Materials (FAA), Fabrics in the Passenger Rail Cars and Locomotive Cabs (FRA), and Seating Upholstery in Buses and Vans (FTA)

This test methodology is intended for use in determining the resistance of materials to flame when tested according to the 60-second and 12-second vertical Bunsen burner tests specified in the FRA [2].

The test is performed in a draft free cabinet using specimens at least 3 x 12-inches (75 x 305-mm) unless the actual size used is smaller. Bunsen burner flame is applied at the bottom of the vertical sample for either 60 seconds or 12 seconds.

The requirements for the specimens are: 1) average flame time will not exceed 15 seconds (FAA) or 10 seconds (FRA and FTA) for either 12 or 60-second exposure; 2) average drip extinguishment time will not exceed 3 seconds for the 60-second exposure or 5-second for the 12-second exposure, and 3) burn length will not exceed 6-inches (152-mm) (FAA, FRA, FTA) for the 60-second and 8-inches (203-mm) for the 12-second exposure.

3-1-6. FAR 25.853: Bunsen Burner Test for Horizontal Aircraft Cabin, Cargo Compartment and Miscellaneous Materials

This test methodology is intended for use in determining the resistance of materials to flame when tested according to 15-second horizontal Bunsen burner tests specified in the FAR 25.853 [2].

The test is the same as the vertical test, except that the specimen is horizontal and is exposed to the burner for 15 seconds. Burn rate is measured in the test. The requirements for the specimens are that the burn rates will not exceed 2.5 inches/min (FAR 25.853(b-2) or 4 inches/min for FAR 25.853 (B-3).

3-1-7. FAR 25.853: Heat Release Rate for Cabin Materials

This test is intended for use in determining heat release rates to show compliance with the requirements of FAR 25.853 [2]. The Ohio State University (OSU) Heat Release Rate Apparatus is used in this standard, which is also a ASTM standard [6].

In the test 5.94- x 5.94-in (150- x 150-mm) and up to 1.75-in (45-mm) thick specimens are wrapped in a 0.03-mm thick aluminum foil. The sample orientation is variable. The sample is exposed to 35 kW/m^2 of radiant heat flux for 5-minutes and heat release rate is measured.

The requirements for the specimens are that the average heat release rate will not exceed 65 kW/m^2 during the 5-minute tests and that the total heat release rate during the first 2-minutes will not exceed 65 $kW\text{-}min/m^2$.

3.2 TEST METHODS SPECIFIED FOR TESTING OF MATERIALS BY VARIOUS AGENCIES AND TESTING LABORATORIES

There are several standard test methods specified for testing of materials [7,8, 9,10,11,12,13,14,15,16,17].

3-2-1 ASTM D2863-70 Test Method for the Limited Oxygen Index of Materials

Minimum oxygen concentration at or below which there is no downward fire propagation for a vertical sheet of a material inside a glass cylinder, with gas flowing in an upward direction, is considered to be a characteristic property of the material in the ASTM D2863 Oxygen Index Test Methodology [9]. In the test, minimum oxygen concentration at which there is downward fire propagation over a small vertical sheet of material is determined and defined as the *Limited Oxygen Index (LOI)* of the material. The vertical sample used is 2.8 to 5.9-in (70 to 150-mm) in length, 0.26-in (6.5-mm) in width and 0.12-in (3-mm) in thickness. Examples of the LOI values for selected materials, taken from Refs. 18 and 19 are listed in Table 3-2.

3-2-2 ASTM E1321-97a (LIFT) Test Methodology to Determine Ignition and Flame Spread Properties of Materials

This test method determines material properties related to piloted ignition of a vertically oriented sample under a constant and uniform heat flux and to lateral flame spread on a vertical surface due to an externally applied radiant-heat flux [10,20,21]. For the ignition test, 6.1-in (155-mm) x 6.1-in (155-mm) thermally thick samples are exposed to a nearly uniform heat flux and the time to flame attachment, using piloted ignition is determined.

Table 3-2. Limiting Oxygen Index of Materials [18,19]

Material	LOI	Material	LOI
Cotton	16 - 17	Polyvinylfluoride (Tedlar®)	22.6
Filter paper	18.2	Polyvinylidenefluoride (Kynar®)	39.0
Plywood	23.0	Polytetrafluoroethylene (Teflon®)	95.0
Cellulose acetate	16.8	Neoprene	40.0
Rayon	18.7-18.9	Polyisoprene	18.5
Wool	23.8	Neoprene rubber	26.3
Polyethylene	17.4	Natural rubber foam	17.2
Polyethylene +50 % Al_2O_3	19.6	Leather	34.8
Polyethylene + 20 % Chlorine	24.5	Polyester fabric	20.6
Polypropylene	17.4	Polyester + 70% glass fiber (25 ^oC)	28.0
Polystyrene	17.8-18.3	Polyester + 70% glass fiber (300 ^oC)	<10.0
Nylon 6,6	24.3-29.0	Epoxy	19.8
Polyimide (Kapton®)	36.5	Epoxy + 65 % glass fiber (25 ^oC)	38.0
Polyacrylonitrile	18.0	Epoxy + 65 % glass fiber (300 ^oC)	16.0
ABS	18.3-18.8	Phenolic	21.0
ABS + 20 % fiber glass	21.6	Phenolic + 80% glass fiber (25 ^oC)	53.0
Polyoxymethylene(Delrin®)	14.9	Phenolic + 80% glass fiber (100 ^oC)	98.0
Polymethylmethacrylate	17.3	Phenolic + 80% Kevlar® (25 ^oC)	28.0
Polycarbonate	22.5-28.0	Phenolic + 80% Kevlar® (300 ^oC)	26.0
Polyacetal (Celcon®)	14.9	Silicone rubber (RTV, etc)	23.0-36.0
Polysulfone	30.0-32.0	Silicone grease	26.0
Nomex®	28.5	Fluorosilicone grease	30.5-68.0
PVC (rigid)	45.0-49.0	Fluorocarbon rubber (Viton® etc)	40.5-60.5
Polyurethane foam	16.5	Balston® Filters	42.5-47.0
SBR foam	16.9	Chlorotrifluoroethylene lubricants	67.0-75.0
PVC (chlorinated)	45.0-60.0	Fluorocarbon (FEP/PFA) tubing	77.0-100.0
Polytrichlorofluorethylene (Kel-F®)	95.0		
Polyvinylidenechloride (Saran®)	60.0		

For the flame spread test, 6.1-in (155-mm) wide and 31.4-in (800-mm) long thermally thick sample is exposed to a graduated heat flux that is approximately 5 kW/m^2 higher at the hot end than the minimum heat flux necessary for ignition (determined from the ignition test).

The test results provide a minimum surface flux and temperature necessary for ignition ($\dot{\mathbf{q}}''_{\mathbf{o,ig}}$, $\mathbf{T_{ig}}$) and for lateral spread ($\dot{\mathbf{q}}''_{\mathbf{o,S}}$, $\mathbf{T_{s,min}}$), an effective material thermal inertia value ($\mathbf{k\rho c_p}$) and a flame-heating parameter ($\mathbf{\Phi}$) pertinent to lateral flame spread (**k** is the thermal conductivity

of the material in kW/m-K, ρ is the density of the material in g/m^3 and $\mathbf{c_p}$ is the heat capacity in kJ/g-K):

$$\mathbf{V_{p(t)}^{-1/2} = C^{-1/2}(\dot{q}''_{o,ig} - \dot{q}''_e F(t))} \quad (2)$$

where $\mathbf{V_{p(t)}}$ is the flame spread rate at time (mm/s); **C** is the flame spread parameter, expressed as $\mathbf{(h^2\Phi / k\rho c)^{-1/2}}$, $\dot{\mathbf{q}}''_{\mathbf{e}}$ is the external heat flux (kW/m^2), and **F(t)** is the ratio of the heat flux at flame arrival position to flame heat flux at 50-mm in the Apparatus, **h** is the heat loss coefficient (kW/m^2-K). From the plot of $\mathbf{V_{p(t)}^{-1/2}}$ against $\dot{\mathbf{q}}''_{\mathbf{e}}\mathbf{F(t)}$, the following are determined: 1) **C** from the slope, 2) $\dot{\mathbf{q}}''_{\mathbf{o,ig}}$ from the x-intercept, 3) $\mathbf{T_{ig}}$ value from $\dot{\mathbf{q}}''_{\mathbf{o,ig}}$ and theoretical curve for surface temperature, 5) $\dot{\mathbf{q}}''_{\mathbf{s,min}}$ value from the position where flame stops and 6) $\mathbf{T_{s/min}}$ from the $\dot{\mathbf{q}}''_{\mathbf{s,min}}$ value and the theoretical curve for surface temperature.

An examination of the data for ignition temperature, $\mathbf{T_{ig}}$, and minimum temperature for flame spread, $\mathbf{T_{s,\,min}}$ shows that there is a relationship between the two temperatures. A similar relationship exists between, $\dot{\mathbf{q}}''_{\mathbf{s,min}}$, and minimum heat flux for ignition, defined as the critical heat flux, $\dot{\mathbf{q}}''_{\mathbf{o,ig}}$.

3-2-3 ASTM E1354 Test Methodology for the Release of Heat and Smoke (The Cone Calorimeter

In the test methodology, 4-in (100-mm) x 4-in (100-mm) horizontal samples are exposed to external heat flux in the presence of a pilot in normal air [11,22,23]. Measurements are made for time to ignition, release rates of heat and products, and mass loss rate.

Automotive materials from the passenger compartment of selected automobiles have been tested in the Cone Calorimeter [22,23]. Data are presented in terms of the following parameters (see Volume III):

- Pk RHR, Av RHR and RHR 3: peak and average heat release rate for the entire test and 3 minutes following ignition (kW/m^2);
- Fire performance index (time-to-ignition/peak heat release rate) (sm^2/kW);
- Ht Comb: effective heat of combustion (MJ/kg); MsLs: mass loss (g or %);
- Pk RSR: peak rate of smoke release (volumetric flow rate in m^3/s x optical density in 1/m / {sample area (0.0100 m^2) x light path length (0.1095-m)} (1/s);
- SEA: specific extinction area (m^2/kg);

- SmkFct: smoke factor [total smoke released x peak heat release rate](MW/m^2);
- THR: total heat release rate (MJ/m^2);
- TSR: total smoke released;
- TTI: time-to-ignition (s); TTE: time-to-extinction (s).

The Fire Propagation Index (**FPI**) considered to be a useful parameter to assess the flame spread behavior of materials [13,15,16,17,18,24,25] cannot be measured reliably in the Cone Calorimeter as normal air is used in the tests [26].

3.2.4 ASTM E2058 Test Methodology for Ignition, Combustion, Flame Spread, and Release of Heat and Chemical Compounds Including Smoke

In the test methodology for ignition, combustion and release of heat and chemical compounds including smoke, 4-in (100-mm) x 4-in (100-mm) square or 4-in (100-mm) diameter round horizontal sample with thickness > 0.12-in (3-mm) is used [13,15,16,17,18,24]. The sample is exposed to external heat flux in the presence of a pilot in normal air and in air with variable flow rate and oxygen concentration. In the flame spread test, 4-in (100-mm) wide and 12-in (305-mm) long vertical sample with thickness > 0.12-in (3-mm) is exposed to heat flux at the bottom in air with 40% oxygen concentration, flowing vertically around the sample [13,15,16,17,18,24].

In the tests for ignition, combustion, release of heat and chemical compounds including smoke, and flame spread, measurements are made at various external heat flux values and air flow rate around the sample for:

1) Time to ignition
2) Weight loss;
3) Concentrations of products and oxygen
4) Ambient and hot gas temperatures;
5) Total volumetric (mass) flow rate of product-air mixture through the sampling duct;
6) Optical transmission through the product-air mixture flowing through the sampling duct;
7) Initial and final weight of the sample;
8) Visual observations (flame height and color, smoke particulate shape, size, and color, melting and charring behaviors of the sample).

The measured data are used to calculate the following (the theory is discussed in Chapter I and in Volume III):

1) Critical heat flux (**CHF**) and Thermal Response Parameter (**TRP**): they characterize the ignition resistance of a material;

2) Release rates of heat and chemical compounds including smoke, heat of combustion, yields of chemical compounds and Heat Release Parameter (**HRP**): they characterize the combustion behavior of a material;
3) Fire Propagation Index (**FPI**): it characterizes the flame spread behavior of a material (see Section 3-2-6).

3-2-5. UL94 STANDARD TEST METHOD FOR THE FLAMMABILITY OF PLASTIC MATERIALS FOR PARTS IN DEVICES AND APPLIANCES

In this test methodology, both horizontal burning (**HB**) and vertical burning (**V**) behaviors of materials are examined [14]. For horizontal burning test for classifying materials 94HB, 5-in (127-mm) long and 0.5-in (12.7-mm) wide samples with maximum thickness of 0.5-in (12.7-mm) are placed on top of wire gauge and ignited by a 30-seoncd exposure to a Bunsen burner at one end. For 94HB materials: 1) the burning rate does not exceed 1.5 in/min (38.1-mm/ min) over a 3.0-in (76.2-mm) specimen having a thickness of 0.120-0.500-in (3.05 to 12.7-mm), 2) the burning rate does not exceed 3.0-in/min (76-mm/min) over a 3.0-in (76-mm) span for specimen having thickness less than 0.120-in (3.05-mm), or 3) cease to burn before reaching 4.0-in (102-mm).

For classifying materials as 94V-0, 94V-1, or 94V-2 in the vertical burning test, 5-in (127-mm) long and 0.5-in (12.7-mm) wide specimens with thickness limited to 0.5-in (12.7-mm) are used. The bottom edge of the specimen is ignited by 5-second exposure to a Bunsen burner with a 5-second delay and repeated five times until the sample ignites. The 94V-0, 94V-1, and 94V-2 material classification criteria are listed in Table 3-3.

Table 3-3. UL 94 V-0, V-1, and V-2 Classification of Materials

Criterion	94V-0	94V-1	94V-2
A. Flaming combustion time after removal of the test flame (s)	≤ 10	≤ 30	≤30
B. Total flaming combustion time after 10 test flame applications for each set of five specimens (s)	≤50	≤ 250	≤ 250
C. Burning with flaming or glowing combustion up to the holding clamp	No	No	No
D. Dripping flaming particles that ignite the dry absorbent surgical cotton located 12-in (305-mm) below the test specimen	None	None	Yes
E. Glowing combustion persisting for more than 30 seconds after the second removal of the test flame (s)	None	≤ 60	≤ 60

The relative resistance of materials to burning according to UL94 is HB < V-2 < V-1 < V-0. Examples of the UL94 classification of materials are listed in Table 3-4 along with their peak pyrolysis or decomposition temperature ($\mathbf{T_p}$ or $\mathbf{T_d}$), pyrolysis residue, and Limiting Oxygen

Index (**LOI)** values, where data are taken from the FAA research study on polymers for aircraft [27].

Table 3-4. Peak Pyrolysis or Decomposition Temperature (T_p or T_d), Pyrolysis Residue, Limiting Oxygen Index (LOI), and UL Ranking for Materials

Polymer	T_p or T_d (^oC)	Residue (%)	LOI (%)	UL 94 Ranking
Polybenzobisoxazole (PBO)	789	75	56	V-0
Polyparaphenylene	652	75	55	V-0
Polybenzimidazole (PBI)	630	70	42	V-0
Polyamideimide (PAI)	628	55	45	V-0
Polyaramide (Kevlar)	628	43	28	V-0
Polyetherketoneketone (PEKK)	619	62	40	V-0
Polyetherketone (PEK)	614	56	40	V-0
Polytetrafluoroethylene (PTFE)	612	0	95	V-0
Polyetheretherketone (PEEK)	606	50	35	V-0
Polyphenylsulfone (PPSF)	606	44	38	V-0
Polypara(benzoyl)phenylene (PX)	602	66	41	V-0
Fluorinated Cyanate Ester	583	44	40	V-0
Polyphenylenesulfide (PPS)	578	45	44	V-0
Polyetherimide (PEI)	575	52	47	V-0
Polypyromellitimide (PI)	567	70	37	V-0
Liquid Crystal Polyester	564	38	40	V-0
Polycarbonate (PC)	546	25	26	V-2
Polysulfone (PSF)	537	30	30	V-1
Polyethylene (PE)	505	0	18	HB
Polyamide 6 (PA6)	497	1	21	HB
Polyethylenenaphthalate (PEN)	495	24	32	V-2
Polyphthalamide	488	3	22	HB
Phenolic Triazine Cyanate Ester (PT)	480	62	30	V-0
Polyethyleneterephthalate (PET)	474	13	21	HB
Cyanate ester of Bisphenol-A (BCE)	470	33	24	V-1
Polydimethylsiloxane (PDMS)	444	0	30	HB
Acrylonitrile-butadiene-styrene (ABS)	444	0	18	HB
Polyurethane elastomer (PU)	422	3	17	HB
Polymethylmethacrylate (PMMA)	398	2	17	HB
Polychlorotrifluoroethylene (PCTFE)	380	0	95	V-0
Polystyrene (PS)	364	0	18	HB
Polyoxymethylene (POM)	361	0	15	HB
Poly(a-methylstyrene)	341	0	18	HB
Polyvinylchloride (PVC)	270	11	50	V-0

3-2-6. FM Approval's Test Methodology to Determine Material Flammability Characteristics Related To Fire Propagation and Smoke Release: Class 4910, 3972, and 4998

In this methodology, ignition, combustion, and fire propagation tests are performed to assess the ignition, fire propagation, and smoke release behaviors of materials [15,16,17,25]. For defining the fire propagation behavior, the Fire Propagation Index (**FPI**) is used:

$$\mathbf{FPI} = 1000\left(\left(0.42\dot{Q}'_{ch}\right)^{1/3} \Big/ \mathbf{TRP}\right) = 750\,(Q'_{ch})^{1/3}/\mathbf{TRP} \tag{3}$$

where $\dot{Q}'_{ch}$ is the chemical (actual) heat release rate for upward fire propagation per unit width of the sample (kW/m) and

$$\mathbf{TRP} = \Delta T_{ig}\left(\pi k \rho c_p / 4\right)^{1/2} \tag{4}$$

ΔT_{ig} is the ignition temperature of the polymeric material above ambient (K), **k** is the thermal conductivity of the polymeric material (kW/m-K), ρ is the density of the polymeric material (g/m^3), and c_p is the heat capacity of the polymeric material (kJ/g-K).

In the test methodology, $\dot{Q}'_{ch}$ is measured during the upward fire propagation on the surface of a vertical specimen 4-in (100-mm) in width and 12-in (303-mm) in height and between 0.1- to 0.5-in (3- to 13-mm) in thickness. The specimen is kept inside a quartz tube such that flow of air with 40 % oxygen concentration surrounds the specimen. **TRP** is determined from the ignition tests by measuring time-to-ignition at various heat flux values. The relationship between the **FPI** values determined from the ASTM E 2058 apparatus and fire propagation behavior is established in the large-scale parallel tests.

Smoke is measured in the combustion test and the yield of smoke multiplied by **FPI**, defined as the Smoke Development Index (**SDI**) is used to assess the release of smoke. Table 3-5 lists some examples of the **FPI, SDI** and yield of smoke (y_s) values.

In the test methodology used for clean room materials [25], electrical cables [16], and conveyor belts [17], the material acceptance criteria are:

- *Polymers for Clean Rooms of the Semi-Conductor Industry*: **FPI** $\leq$ 6 $(m/s^{1/2})/(kW/m)^{2/3}$ and **SDI** $\leq$ 0.4 $(g/g)(m/s^{1/2})/(kW/m)^{2/3}$;
- *Electrical Cables:*
  - Group 1 cables (non-self sustained flame propagation): **FPI** < 10 $(m/s^{1/2})/(kW/m)^{2/3}$;
  - Group 2 cables (self-sustained flame propagation): 10 <**FPI** < 20 $(m/s^{1/2})/(kW/m)^{2/3}$;
  - Group 3 cables (rapid self-sustained flame propagation): **FPI** $\geq$ 20 $(m/s^{1/2})/(kW/m)^{2/3}$
- *Conveyor Belts*: **FPI** $\leq$ 7 $(m/s^{1/2})/(kW/m)^{2/3}$

Table 3-5. Smoke Development Index (SDI), Visual Observations, Yield of Smoke (y_s) and Fire Propagation Index (FPI) values for Various Materials

Polymeric Materials	FPI[a]	SDI[b]	y_s[c]	Smoke Amounts and Color (Visual)
Polystyrene	34	5.60	0.165	Copious, black
PVC-PVC cable	36	4.10	0.114	Copious, black
PE-PVC cable	28	3.80	0.136	Copious, black
Polybutyleneterphthalate	32	2.20	0.069	Copious, black
Fire retarded-polypropylene	30	2.10	0.070	Copious, black
Polycarbonate	14	2.10	0.150	Copious, black
Silicone-PVC cable	17	2.00	0.118	Copious, black
Polypropylene	32	1.76	0.055	Very large, black
PE-25% chlorine	15	1.70	0.113	Very large, black
PVC (flexible)	16	1.60	0.100	Very large, black
Polyphenyleneoxide	9	1.60	0.178	Very large, black
PE-36% Cl	11	1.50	0.136	Large, black
PE-48% Cl	8	1.42	0.178	Large, black
Acrylonitrile-butadiene-styrene	8	0.80	0.100	Small, black
PVC-D (rigid)	7	0.70	0.100	Small, grayish
Polymethylmethacrylate	31	0.62	0.020	Small, light grayish
Polyetheretherketone, PEEK-1	6	0.40	0.067	Very small, grayish-white
PVC-E rigid	6	0.30	0.050	Very small, grayish-white
PVC-F (rigid)	4	0.30	0.075	Very small, grayish-white
Polyetherimide	8	0.15	0.019	Very small, grayish-white
Wood slab	14	0.20	0.014	Very small, grayish-white
Polyvinylidenefluoride	4	0.12	0.030	Very small, grayish-white
Polyoxymethylene	15	0.03	0.002	Very small, grayish-white
PEEK-2	4	0.03	0.008	Very small, grayish-white
PTFE, Teflon®	4	0.01	0.003	Very small, grayish-white

a: $(m/s^{1/2})/(kW/m)^{2/3}$; **b**: $(g/g)(m/s^{1/2})/(kW/m)^{2/3}$; **c**: yield of smoke (g/g)

REFERENCES

1. Number 571.302. Standard No. 302: Flammability of Interior Materials, 49CFR Ch.V (10-1-98 Edition), 1998.

2. Aircraft Materials Fire Test Handbook, Final Report DOT/FAA/AR-00/12, Federal Aviation Administration, April 2000.

3. "Test Procedures and Performance Criteria for the Flammability and Smoke Emission Characteristics of Materials Used in Passenger Cars and Locomotive Cabs", Federal Register, Rules and Regulations, Volume 64, No. 91, Wednesday, May 12, 1999.

4. Department of Transportation, Federal Transit Administration, Docket 90-A "Recommended Fire Safety Practices for Transit Bus and Van Materials Selection", Federal Register, Volume 58, No. 201, Wednesday, October 20, 1993.

5. Grenier, A.T., and Maguire, P.J., "Maritime Fire Safety Standards - Some Insight from an AHJ", Maritime Fire Safety Standards, U.S. Coast Guard, Washington, DC.

6. ASTM E906-83, "Standard Test Method for Heat and Visible Smoke Release Rates for Materials and Products", The American Society for Testing and Materials, West Conshohocken, PA. 1984.

7. Docket Number: NHTSA-1998-3588-84 (Abu-Isa, I.A., and Shehdeh, J., "Thermal Properties of Automotive Polymers. III: Thermal Characteristics and Flammability of Fire Retardant Polymers"), June 27, 2000.

8. Docket Number: NHTSA-1998-3588-104 (Abu-Isa, I.A., Shehdeh, J., and LaDue, D., "Thermal Properties of Automotive Polymers IV. Thermal Gravimetric Analysis and Differential Scanning Calorimetry of Selected Parts from a Chevrolet Camaro", June 2000

9. ASTM D 2863-70, "Standard Test Method for Flammability of Plastics Using the Oxygen Index Method", American Society for Testing and Materials, West Conshohocken, PA 1970.

10. ASTM E 1321-97a, "Standard Test Method for Determining Material Ignition and Flame Spread Properties", American Society for Testing and Materials, West Conshohocken, Pa. 1997.

11. ASTM E1354-90, "Standard Test Method for Heat and Visible Smoke Release Rates for Materials and Products Using Oxygen Consumption Calorimeter", The American Society for Testing and Materials, West Conshohocken, PA. 1990.

12. ASTM E906-83, "Standard Test Method for Heat and Visible Smoke Release Rates for Materials and Products", The American Society for Testing and Materials, West Conshohocken, PA 1984.

13. ASTM E 2058-01, "Standard Test Methods for Measurement of Synthetic Polymer Flammability Using a Fire Propagation Apparatus (FPA)", American Society for Testing and Materials, West Conshohocken, PA 2001.

14. UL 94, "Standard for Tests for Flammability of Plastics Materials for Parts in Devices and Appliances", Third Edition. Underwriters Laboratories Inc., Northbrook, IL. June 12, 1989.

15. FMRC Class Number 4910, "Test Standard, Clean Room Materials Flammability Test Protocol", Factory Mutual Research Corporation, Norwood, MA, September 1997.

16. FMRC Class 3972, "Specification Standard for Cable Fire Propagation", Factory Mutual Research Corporation, Norwood, MA, 1989.

17. FMRC Class 4998, "Approval Standard Class 1 Conveyor Belting", Factory Mutual Research Corporation, Norwood, MA, 1995.

18. Tewarson, A., 1996. "Flammability", Chapter 42 in the *Physical Properties of Polymers Handbook (*J.E. Mark, Editor), pp. 577-604. The American Institute of Physics, Woodbury, N.Y.

19. NFPA 53, 1999 Edition, "Recommended Practice on Materials, Equipment, and Systems Used in Oxygen-Enriched Atmospheres", National Fire Protection Association, Quincy, MA. 1999.

20. Quintiere, J.G., "Principles of Fire Behavior", Delmar Publishers, New York, N.Y. 1997.

21. Quintiere, J.G., "Surface Flame Spread", The SFPE Handbook of Fire Protection Engineering, Society of Fire Protection Engineering, National Fire Protection Association, 2nd Edition, Section 2, Chapter 14, pp. 2-205 to 2-216, 1995.

22. Hirschler, M.M. "Fire Hazard of Automotive Interiors", Proceedings Fire Risk and Hazard Assessment Research Application Symposium-Research & Practice: Bridging the Gap. pp.164-195. June 24-26, 1998, San Francisco, CA. National Fire Protection Research Foundation, NFPA, Quincy, MA.

23. Battipaglia, K.C., Griffith, A.L., Huczek, J.P., Janssens, M.L., Miller, M.A., and Willson K., "Comparison of Fire Properties of Automotive Materials and Evaluation of Performance Levels", Final Report Project 01.05804, Southwest Research Institute, San Antonio, Texas, October 2003.

24. Tewarson, A., "Generation of Heat and Chemical Compounds in Fires", Section 3, Chapter 3-4, pp. 3-82 to 3-161. The SFPE Handbook of Fire Protection Engineering, Third Edition, National Fire Protection Association Press, Quincy, MA, 2002.

25. Tewarson, A., Khan, M.M., Wu, P.K., and Bill, R.G., "Flammability Evaluation of Clean Room Polymeric Materials for the Semi Conductor Industry", *Fire & Materials*, **25**, 31-42, 2001.

26. Wu, P.K., and Bill, R.G., "Laboratory Tests for Flammability Using Enhanced Oxygen", Fire Safety Journal, 38, 203-217, 2003.

27. Lyon, R.E., "Solid-State Thermochemistry of Flaming Combustion", Final Report DOT/FAA/AR-99/56. U.S. Department of Transportation, Federal Aviation Administration, Office of Aviation Research, Washington, D.C. July 1999.